Accepted Manuscript

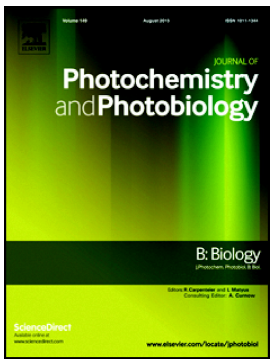

Spectroscopic characterizations, structural peculiarities, molecular docking study and evaluation of biological potential of newly designed organotin(IV) carboxylates

Muhammad Sirajuddin, Saqib Ali, Vickie McKee, Naheed Akhtar, Saiqa Andleeb, Abdul Wadood

PII: S1011-1344(19)30458-0
DOI: https://doi.org/10.1016/j.jphotobiol.2019.111516
Article Number: 111516
Reference: JPB 111516

To appear in: *Journal of Photochemistry & Photobiology, B: Biology*

Received date: 15 April 2019
Revised date: 30 April 2019
Accepted date: 27 May 2019

Please cite this article as: M. Sirajuddin, S. Ali, V. McKee, et al., Spectroscopic characterizations, structural peculiarities, molecular docking study and evaluation of biological potential of newly designed organotin(IV) carboxylates, Journal of Photochemistry & Photobiology, B: Biology, https://doi.org/10.1016/j.jphotobiol.2019.111516

Spectroscopic characterizations, Structural peculiarities, Molecular docking study and evaluation of biological potential of newly designed organotin(IV) carboxylates

Muhammad Sirajuddin[a,*], Saqib Ali[b,*], Vickie McKee[c], Naheed Akhtar[d], Saiqa Andleeb[d], Abdul Wadood[e]

[a] Department of Chemistry, University of Science and Technology Bannu, 28100, Pakistan

[b] Department of Chemistry, Quaid-i-Azam University, Islamabad, 45320, Pakistan

[c] Department of Chemistry, Dublin City University, Ireland, UK

[d] Department of Zoology, University of Azad Jammu and Kashmir, Muzaffarabad 13100, Pakistan.

[e] Department of Biochemistry, Computational Medicinal Chemistry Laboratory, UCSS, Abdul Wali Khan University Mardan, Pakistan

*Corresponding author address: m.siraj09@yahoo.com (M. Sirajuddin); drsa54@hotmail.com (S. Ali)

Abstract

In the search for new therapeutic agents we have synthesized 13 new organotin(IV) carboxylate derivatives of (*E*)-4-((4-methoxy-2-nitrophenyl)amino)-4-oxobut-2-enoic acid. The synthesized complexes were characterized by several spectroscopic techniques. A chelating or bridging bidentate nature of the carboxylate ligand was suggested from the solid state FT-IR results. Solution state multinuclear NMR (^{1}H, ^{13}C and ^{119}Sn) results reveal that the geometry around the Sn atom in triorganotin(IV) complexes is trigonal bipyramidal and in diorganotin(IV) complexes is octahedral. The ligand, (*E*)-4-((4-methoxy-2-nitrophenyl)amino)-4-oxobut-2-enoic acid, complex **1** and complex **2** were also analyzed by single crystal X-ray technique and the results fully supports the spectroscopic data. For **1** and **2** the geometry optimized by the single crystal X-ray analyses is distorted trigonal bipyramidal. The interaction of the studied compounds with SS-DNA was investigated by UV-Vis. Spectroscopy and Molecular docking showing an intercalative mode of binding. The evaluation of the screened compounds for cancer treatment displays even higher than that of the vincristine used as a standard drug. Similarly the performance of the tested compounds as an antileishmanial agent considers them very close in activity to the standard drug, amphotericin B. The antibacterial results show that the most of the compounds have a moderate sensitivity against the studied bacterial pathogens.

Keywords: Organotin(IV) Carboxylate; Spectroscopic Characterization; DNA Interaction Study; Anticancer Activity; Antileishmanial Activity; Molecular docking

1. Introduction

Organometallic compounds which contain Sn atom attached to organic moiety with atleast one direct Sn-C covalent bond are known as organotin(IV) compounds or simply organotins with general formula of R_nSnX_{4-n}; where R is the organic moiety, X is any anionic group like Cl^-, OH^- etc. and n = 1-4. Depending on the number of organic moiety (n) attached to Sn atom the organotin(IV) compounds are classified as: $RSnX_3$, R_2SnX_2, R_3SnX and R_4Sn: and are called mono, di, tri and tetra organotin(IV) compounds, respectively [1]. Organotin(IV) compounds have lot of applications both on non-biological and biological sides. The non-biological applications include effective catalyst in the conversion of oil into biodiesel *via* trans esterification reaction [2-4], antiseptic agents for marine [5], preservatives for wood [6, 7], antifouling paints [8], polymer stabilizers [9], curing of silicon, and so forth [10, 11].

On the other hand the biological side covers the vast field of medicinal chemistry due to their structural diversity and large therapeutic applications [12].

Cancer, which is also known as deadly fatal disease, is the 2nd most common disease after the cardiovascular disease and is major issue to the human being from a very long time. The cancer affected patients are increased day by day mainly due the modernization of the society. There are many available anti cancer drugs in the markets but they posses some serious side effects that bound their use for affective treatment. Due to these factors the demand for new affective and less costly drugs is still continued [13].

Anticancer compounds must interact with DNA to stop its replication or transcription by different ways, although the exact mechanism is till under the investigation [14]. The study of DNA interaction with organotin(IV) compounds received incredible researcher attention from the last few years as a result of their good anticancer and antitumor activities [11]. Metal oxidation state, coordinated ligands, coordination number and geometry mostly affect the target recognition [15]. DNA is the easy target for the organotins due to their specificity for DNA sequences resulting in the alteration of the DNA structure leading to the inhibition of the protein activator or repressor and ultimately influences the gene expression process [16]. The organotin(IV) compounds have the ability of interaction with DNA which depends on number of

factors like: geometry of the molecule or coordination number of the Sn atom, nature of the organic moiety already attached to the Sn atom, nature of the coordinated ligand and ease of the ligand hydrolysis [11, 17]. Organotin(IV) compounds interact with DNA *via* different modes such interaction (in which the planar part of the molecule insert into the DNA bases), groove binding (in which the compound with L type structure fit itself in the grooves of DNA) and electrostatic interaction [18].

In the context here we are exploring the designing of 13 new organotin(IV) derivatives based on (*E*)-4-((4-methoxy-2-nitrophenyl)amino)-4-oxobut-2-enoic acid. Different instrumental techniques were used for the characterization of the newly synthesized compounds. The biological potential of the synthesized compounds were explored against bacteria, DNA, cancer and leishmania.

2. Experimental section

2.1. Materials and methods

Reagent grade quality chemicals were obtained from chemical companies (Aldrich and E. Merck). The required solvents were 1st dried prior to use in accordance to the reported method [19]. The $(C_6H_5\text{-}CH_2)_2SnCl_2$ salt was synthesized according to the earlier reported method [20]. Salmon fish sperm DNA (SS-DNA) was purchased from Arcos chemical company in the form of solid Na^+ salt and was used as received.

The following instrument/apparatus were used for the desired purpose: Gallenkamp (UK) electrothermal melting point apparatus for melting point determination; Thermo Nicolet-6700 FT-IR Spectrophotometer for FT-IR spectra recording; CE-440 Elemental Analyzer for carbon, hydrogen and nitrogen contents measurement; JEOL ECS instrument (400 MHz) for NMR spectra recording; Shimadzu 1800 UV-Vis. Spectrophotometer for recording absorption spectra of compound-DNA adduct; Bruker Apex II CCD diffractometer for recording the crystal data; Thermo Scientific executive mass spectrometer for recording the mass spectra.

Synthesis

Synthesis of (*E*)-4-((4-methoxy-2-nitrophenyl)amino)-4-oxobut-2-enoic acid (HL)

(*E*)-4-((4-methoxy-2-nitrophenyl)amino)-4-oxobut-2-enoic acid (HL) was prepared by reacting 10 mmol (2.66 g) of 4-methoxy-2-nitroaniline dissolved in glacial CH_3COOH with 10 mmol

(0.98 g) maleic anhydride dissolved in glacial CH_3COOH (Scheme 1) according to our earlier reported procedure [21].

Synthesis of Sodium (*E*)-4-((4-methoxy-2-nitrophenyl)amino)-4-oxobut-2-enoate (NaL)

Sodium (*E*)-4-((4-methoxy-2-nitrophenyl)amino)-4-oxobut-2-enoate (NaL) was prepared by reacting the aqueous solution of sodium hydrogen carbonate ($NaHCO_3$) with suspended solution of (*E*)-4-((4-methoxy-2-nitrophenyl)amino)-4-oxobut-2-enoic acid in distilled water. After mixing the reactants and stirring them at room temperature, a clear solution was obtained that on rotary evaporation of the solvent gives the desired NaL product [22] as shown in Scheme 1.

Synthesis of complexes

Sodium (*E*)-4-((4-methoxy-2-nitrophenyl)amino)-4-oxobut-2-enoate (NaL) was used for the preparation of complexes while reacting with different salts of organotins in different molar ratio of NaL and organotin(IV) chlorides in dried toluene solvent and refluxing for 6-8 hours. i.e., for the synthesis of triorganotin(IV) complexes the molar ratio of NaL and R_3SnCl (R = CH_3, C_2H_5, C_4H_9, C_6H_5 and C_6H_{11}) was 1:1 while for the synthesis of diorganotin(IV) complexes the molar ratio of NaL and R_2SnCl_2 (R = CH_3, C_4H_9, C_6H_5, C_6H_5-CH_2 and C_2H_3) was 2:1. Dioctyltin complex was prepared with the same molar ratio while using HL instead of NaL and $(C_8H_{17})_2SnO$ (Scheme 1) [22]. After the completion of reaction the reaction mixture was filtered to remove the byproduct NaCl and the toluene was evaporated by rotavapor to get the required product which was then recrystallized in chloroform at room temperature.

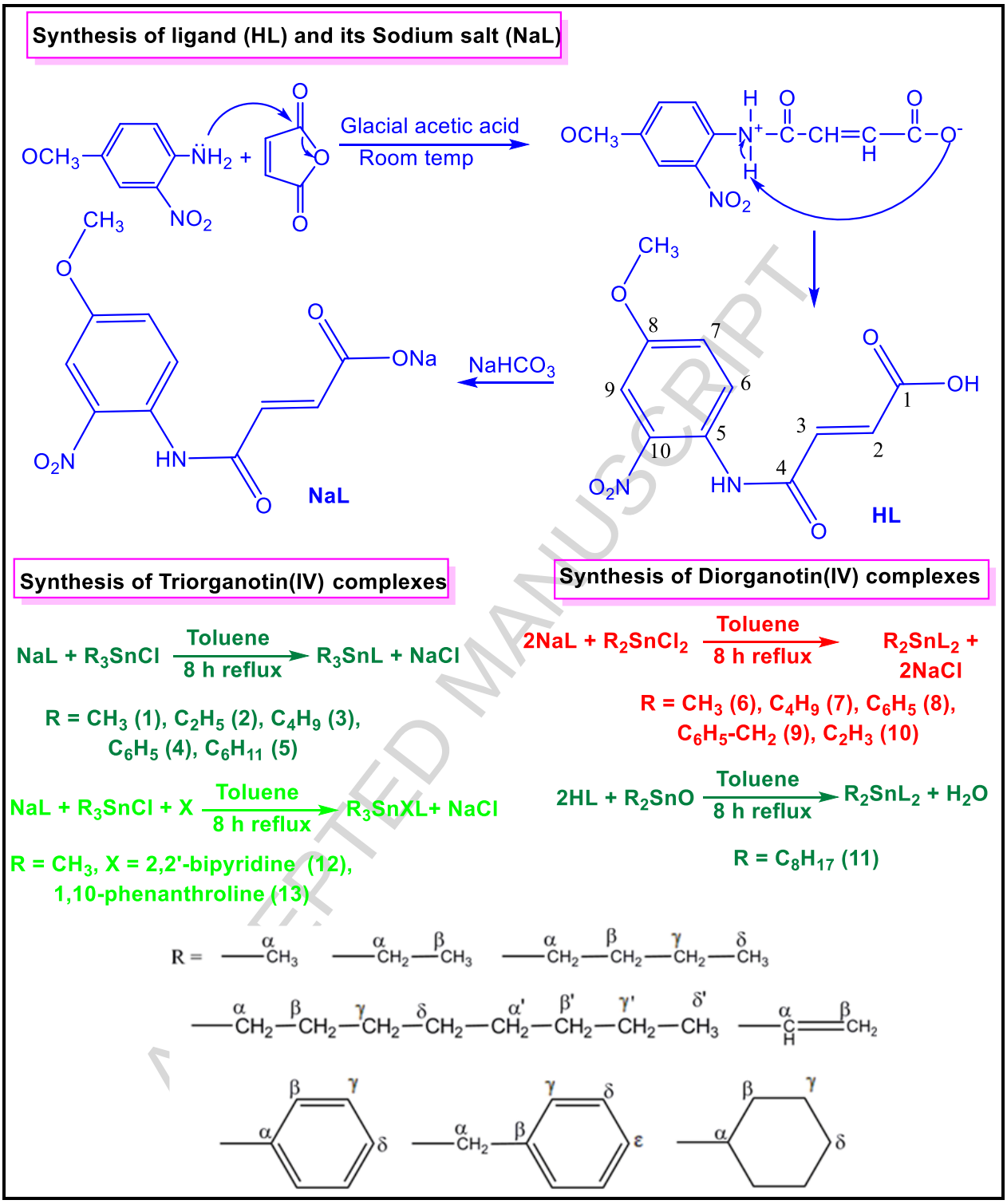

Scheme 1: Synthetic scheme for the preparation of HL, NaL and organotin(IV) complexes along with atom numbering of HL and organic moieties attached to Sn atom

2.2. Electronic absorption titration for DNA binding

Compound-DNA binding was carried out by UV-Vis. Spectroscopy according to the earlier reported method [23, 24]. The tested samples were prepared in 70% ethanol at a concentration of 1 mM. A constant concentration of compounds (1 mM) was treated with varying concentrations of SS-DNA (9-72 µM) at room temperature (25 ± 1 °C). The most shifted peak absorbencies of the compound was noted after the successive additions of DNA. The absorbance of the reference cell was made nil by using the same concentration of DNA in the reference cell also.

2.3. Anticancer Activity

The anticancer potential of the synthesized compounds was evaluated against two cancer cell lines: H-157 and BHK-21 cells according the Skehan's method [25] of SRB (Sulforhodamine B) with some modifications [21, 26]. Different concentrations of compounds were prepared (100, 10, 1 and 0.1 µM) and were transferred to test wells. Control and blank wells were also prepared containing standard drug (Vincristine) and culture media with cells, respectively.

2.4. Antileishmanial activity

The compounds were evaluation of antileishmanial potential against Leishmania major according to the earlier reported method [22, 27]. From different concentrations of compound, 10 µL/well was transferred to triplicate wells. For the antileishmanial activity assays, 100 µL/well of the culture which contained 2.5×10^6 cells/mL promastigotes was seeded in 96-well flat-bottom plates. Then 10 µL/well from various concentrations of compounds were added to triplicate wells and plates were incubated for 72 h at 25 ± 1 °C. The first well of 96 wells was as a blank well which only contained of 100 µL culture medium without any compound, drug or parasite. Amphotericin B was used as standard drug. The experiments were performed in triplicate and results reported in the form of mean of three independent experiments (± SEM) and expressed as percent inhibitions calculated by the formula [22, 27]:

$$\text{Inhibition } (\%) = \left[100 - \frac{\text{absorbance of the test compound}}{\text{absorbance of the control}}\right] \times 100$$

2.5. Antibacterial activity assay

Determination of the antibacterial activity was carried out by agar well-diffusion method [28] against seven human clinical bacterial pathogens *viz.*, *E. coli*, *S. marcesscens*, *K. pneumoniae*, *S. epidermidis*, *S. pyogenes*, *P. aeruginosa* and *S. aureus*. After 24 h, culturing flask containing bacterial strains were poured aseptically in 100 mL flask containing nutrient agar medium, gently

mixed and poured in Petri dishes. Petri plates were allowed to solidify under laminar flow to avoid contamination. Six wells per plate were made with sterile yellow tip of (5mm) and 30 µL of each compound was poured aseptically in wells. For each sample triplicate plates were prepared. After 24 hours incubation at 37 ºC the zone of inhibition around each well was observed and determined using scale in millimeters [29]. Antibacterial activities were calculated as a mean of three replicates. Diameter of the clear zones (> 5 mm) showed bacterial growth around each well [22].

2.6. Molecular docking

MOE "Molecular Operating Environment" (version 2016) [30] software was used for obtaining the 3D figures of the newly synthesized organotin(IV) carboxylates. With the help of 3D protonation, the H atoms to the synthesized compounds were added followed by energy optimization using MOE. Crystal structure of the Salmon sperm-DNA was retrieved using PDB (protein databank) with id: 1BNA) [www.rcsb.org/pdb]. With the help of MOE software (www.chemcomp.com) all the H_2O molecules were eliminated from the retrieved structure of DNA prior to molecular docking. The 3D protonation and energy minimization of the retrieved DNA was performed using MOE software having the default parameters. Docking of the macromolecule (DNA) with the synthesized compounds was done with MOE with default parameters i.e., Placement: Triangle Matcher, Rescoring: London dG. 10 conformations were generated for each compound and the top-ranked conformation of each compound was used for further analysis.

3. Results and discussion

The ligand was synthesized by an easy and economical method by treating aniline and maleic anhydride in beaker at room temperature and within a very short time of 3-5 minutes the precipitate of the resulting compound appeared. The precipitate was washed several times with distilled water and then air dried. The ligand and its organotin(IV) derivative were prepared in good yield and they were both light and air stable in light and dry air. They were freely soluble in solvents such as $CHCl_3$, CH_3OH, C_2H_5OH and $(CH_3)_2SO$ etc. Table 1 presents the %age yield of the product, M.P, CHN (carbon, hydrogen, nitrogen) contents etc of the newly prepared compounds. It can be seen from the data in Table 1 that a very good matching was observed

between the experimentally and theoretically found values of carbon, hydrogen, nitrogen contents.

Table 1: Physical and elemental composition data (%) of the synthesized compounds*

Comp. No	%age Yield	Melting point (°C)	Formula weight	Formula	Carbon, calculated/found	Hydrogen, calculated/found	Nitrogen, calculated/found
HL	93	134-136	266.2	$C_{11}H_{10}N_2O_6$	49.6 (49.5)	3.8 (3.6)	10.5 (10.4)
1	90	151-152	429.0	$C_{14}H_{18}N_2O_6Sn$	39.2 (40.2)	4.2 (4.2)	6.5 (6.6)
2	85	113-115	471.1	$C_{17}H_{24}N_2O_6Sn$	43.0 (42.9)	5.5 (5.5)	5.9 (5.8)
3	76	68-70	555.3	$C_{23}H_{36}N_2O_6Sn$	49.6 (49.7)	6.9 (6.9)	5.1 (5.0)
4	85	80-82	612.2	$C_{29}H_{24}N_2O_6Sn$	56.6 (55.3)	3.9 (4.0)	4.6 (3.8)
5	85	105-107	633.4	$C_{29}H_{42}N_2O_6Sn$	55.0 (54.2)	6.7 (6.5)	4.4 (4.8)
6	75	103-105	679.2	$C_{24}H_{24}N_4O_{12}Sn$	42.4 (38.0)	3.7 (3.9)	8.2 (7.6)
7	80	90-92	763.3	$C_{30}H_{36}N_4O_{12}Sn$	47.2 (47.0)	4.6 (4.2)	7.3 (7.3)
8	80	Paste type	803.3	$C_{34}H_{28}N_4O_{12}Sn$	50.8 (50.3)	3.5 (3.4)	7.0 (7.8)
9	75	Paste type	846.4	$C_{37}H_{35}N_4O_{12}Sn$	52.5 (52.5)	4.2 (3.8)	6.6 (6.2)
10	75	92-94	703.2	$C_{26}H_{24}N_4O_{12}Sn$	44.4 (43.8)	3.4 (3.9)	8.0 (8.4)
11	87	114-116	875.5	$C_{38}H_{52}N_4O_{12}Sn$	52.1 (51.3)	6.0 (6.1)	6.4 (6.2)
12	80	139-141	585.2	$C_{24}H_{26}N_4O_6Sn$	49.3 (49.0)	4.5 (4.2)	9.6 (9.3)
13	78	Paste type	609.2	$C_{26}H_{26}N_4O_6Sn$	51.3 (52.7)	4.3 (4.3)	9.2 (9.3)

* See Schme 1 for compounds numbering

3.1. Solid state FT-IR spectroscopy

Table 2 shows FT-IR data for peaks of our interest such as νOH, νNH, νC=C, νCO, νSn-C, νSn–O and νSn–N. Precious information about synthesis and structural elucidation of the compounds in the solid state can be obtained from the FT-IR data. The disappearance of νOH of the free ligand after treatment with $NaHCO_3$ in the spectrum of the sodium salt confirms the successful formation of NaL. NaL was then used for complexation and coordinates to Sn atom through O atom of the COO group that was confirmed by the presence of new peak for Sn-O in the region of 463-422 cm^{-1} in the spectra of the complexes. This Sn-O peak was absent in the spectrum of the sodium salt of the ligand (NaL). Similarly another important absorption in the region of 551-515 cm^{-1} for C-Sn stretching vibration was observed in the spectra of the complexes. For C_6H_5-Sn derivatives the C-Sn stretching peak was appeared at 282-274 cm^{-1} [22].

Strong absorption bands were observed for symmetric and asymmetric vibrations of the carboxylate moiety in the range of 1380-1340 cm^{-1} and 1532-1501 cm^{-1}, respectively in the spectra of complexes while for the free ligand they appeared at 1317 cm^{-1} and 1539 cm^{-1}. After complexation the value of the symmetric vibration of the carboxylate moiety increases while that of the asymmetric decreases resulting in decrease in difference of the wave number of the asymmetric and symmetric vibrations of the carboxylate moiety 'Δν' [31]. In the spectrum of the NaL the value of Δν is 265 cm^{-1} (Table 2) while that of the complexes is smaller than that of the NaL. The magnitude of the Δν for the reported complexes is less than 200 cm^{-1} which reflects either chelating or bidentate nature of the ligand. The value of Δν was also calculated from single crystal XRD data by using the following equation [32, 33]:

$$\Delta\nu = 1818.1\delta r + 16.47(\theta\mathrm{OCO} - 120) + 66.8$$

The difference between the two C-O bond lengths (Å) is represented by δr and the O-C-O angle (°) is represented by θOCO. After matching the values of Δν obtained both from FT-IR data and crystal data it was found that both the values were in close agreement, i.e., FT-IR data for **HL** and complexes **1** and **2** (222, 160, 153) and single crystal XRD data (224, 133, 136).

Table 2: Selective FT-IR peaks (cm^{-1}) for synthesized compounds*

Comp. #	ν Sn-N	ν Sn-C	ν Sn-O	ν NH	ν C=O	ν (COO) asym	ν (COO) sym	Δν	ν OH
HL	-	-	-	3269	1707	1539	1317	222	3111
NaL	-	-	-	3357	1705	1575	1310	265	-
1	-	545	436	3348	1694	1507	1347	160	-
2	-	515	428	3349	1698	1504	1351	153	-
3	-	538	459	3361	1695	1509	1342	167	-
4	-	282	449	3343	1697	1506	1351	155	-
5	-	540	422	3370	1692	1532	1342	190	-
6	-	542	440	3370	1700	1501	1370	131	-
7	-	527	434	3372	1714	1514	1378	136	-
8	-	274	444	3371	1713	1512	1380	132	-
9	-	543	463	3367	1712	1510	1375	135	-
10	-	545	458	3371	1713	1513	1381	132	-
11	-	544	457	3373	1713	1510	1377	133	-
12	560	546	438	3349	1694	1509	1347	162	-
13	557	551	440	3353	1698	1506	1340	166	-

* See Schme 1 for compounds numbering

3.3. NMR results

3.3.1. ^{1}H NMR

Table 3 presents the data of ^{1}H NMR recorded in DMSO. The ^{1}H NMR spectrum of the ligand shows a peak for the carboxylate OH proton at 13.12 ppm. After complexation this peak was absent in the spectra of the complexes. A *cis* conformation for the H-2 and H-3 protons was confirmed by giving clear doublets with ^{3}J = 12.0-12.4 Hz. H-6 and H-7 protons give doublet while H-9 protons exhibit doublet of doublet. The complextion was further confirmed by the appearance of new Sn-C peak in the spectra of the complexes.

A sharp singlet with clear seattleite peaks at 0.35 ppm was observed for Sn-CH_3 protons in complex **1**. A value of 69 Hz was calculated for $^{2}J[^{119}Sn\text{-}^{1}H]$ which corresponds to the penta-coordinated environment of Sn in solution state [22]. In complex **2** two peaks were observed for the Sn-CH_2-CH_3 protons. A quartet for CH_2 protons (Hα) having $^{2}J[^{119/117}Sn\text{-}^{1}H]$ = 76, 64 Hz was observed while for CH_3 protons (Hβ) a triplet was observed. For Sn-CH_2-CH_2-CH_2-CH_3 protons

(complex **3** & **7**) exhibited a total 4 peaks, i.e., two triplets (Hα & Hδ) and two multiplets (Hβ & Hγ). The Sn-C_6H_5 protons of complex **4** and **8** exhibited total four peaks, i.e., one doublet and two triplets in their respective regions for Hβ, Hγ and Hδ, respectively. The Sn-C_6H_{11} protons of complex **5** exhibited total three peaks, i.e., triplet (Hα), multiplet (Hβ) and broad signals (Hγ & Hδ) in their respective regions. A sharp singlet with clear seattleite peaks at 0.80 ppm was observed for Sn-CH_3 protons in dimethyltin complex (**6**). A value of 100 Hz was calculated for $^2J[^{119}Sn\text{-}^1H]$ which corresponds to the hexa-coordinated environment of Sn in solution state [22, 34]. A singlet peak at 2.04 ppm was observed for the CH_2 protons of the Sn-CH_2-C_6H_5 in complex **9**. A doublet of a doublet was observed in complex **10** for the CH proton of Sn-CH=CH_2 while for the CH_2 protons two doublets with $^3J_{cis}$ (6.0 Hz) $^3J_{trans}$ (9.6 Hz) were observed. A very difficult and complicated type spectra was observed for the $(\text{-}CH_2)_7$ protons of Sn-C_8H_{17} in complex **11**. However a little bit clear triplet was observed for the CH_3 protons.

Lockhart's equation [35] was used for the calculation of C-Sn-C bond angle for the value of $^2J[^{119}Sn\text{-}^1H]$ in complex **1**, **2** and **6** and are shown in Table 5. The observed values of C-Sn-C bond angle in complex **1** and **2** (triorganotin derivatives) show penta-coordinated environment while in complex **6** (diorganotin derivatives) hexa-coordinated environment [36]. Figure 1a presents the spectrum of ^{1}H NMR for complex **1**.

3. 3.2. ^{13}C NMR results

Table 4 presents the complete data for ^{13}C NMR of the synthesized compounds. A downfield shift was observed for the resonances of the carboxylate moiety due to the withdrawal of electron density from ligand by electropositive Sn atom [37]. With respect to free ligand a minor change was observed for the phenyl carbons signals. The position of signal for the Cα in phenyltin complexes (**4** & **8**) falls in the range of 143.5-143.7 ppm which is specified for penta or hexa coordinated environment [22]. The value of C-Sn-C bond angle for methyl and ethyl tin complexes (**1**, **2**, **6**, **12** & **13**) was measured by substituting the value of $^1J[^{119}Sn\text{-}^{13}C]$ in the Lockhart's equation [38]. Howard's equations were for the calculation of C-Sn-C bond angles for butyl and phenyl tin complexes (**3**, **4**, **7** & **8**) [39] and are given in Table 5. The C-Sn-C bond angles calculated from NMR are in good agreement with those obtained from the X-crystallography. For example, for complex **1** the C-Sn-C value obtained from the $^2J(^{119}Sn\text{-}^1H)$

coupling using the Lockhart's equation is 117° while that obtained from crystal data is 118°, respectively. The representative ^{13}C NMR spectrum of the complex **1** is shown in Fig. 1b.

3.3.3. ^{119}Sn NMR results

Table 4 also presents the ^{119}Sn NMR data and all the complexes (1-13) have shown a single peak in their Sn NMR spectra that shows the presence of one specie in solution. For Me_3Sn, Et_3Sn, Bu_3Sn complexes the value of tin NMR was shifted towards highly shielded region (-6.23 to -18.3 ppm) which may be due to the extensive electron donating ability of alkyl groups attached to tin atom [40, 41]. For complex **4**, Ph_3SnL, the ^{119}Sn signal appears at -258.3 ppm. The ^{119}Sn NMR of diorganotin(IV) derivatives lies in the range from -247 ppm to -271.1 ppm which shows hexa-coordinated environment about Sn atom. The ^{119}Sn NMR spectrum of the complex **1** is shown in Fig. 1b.

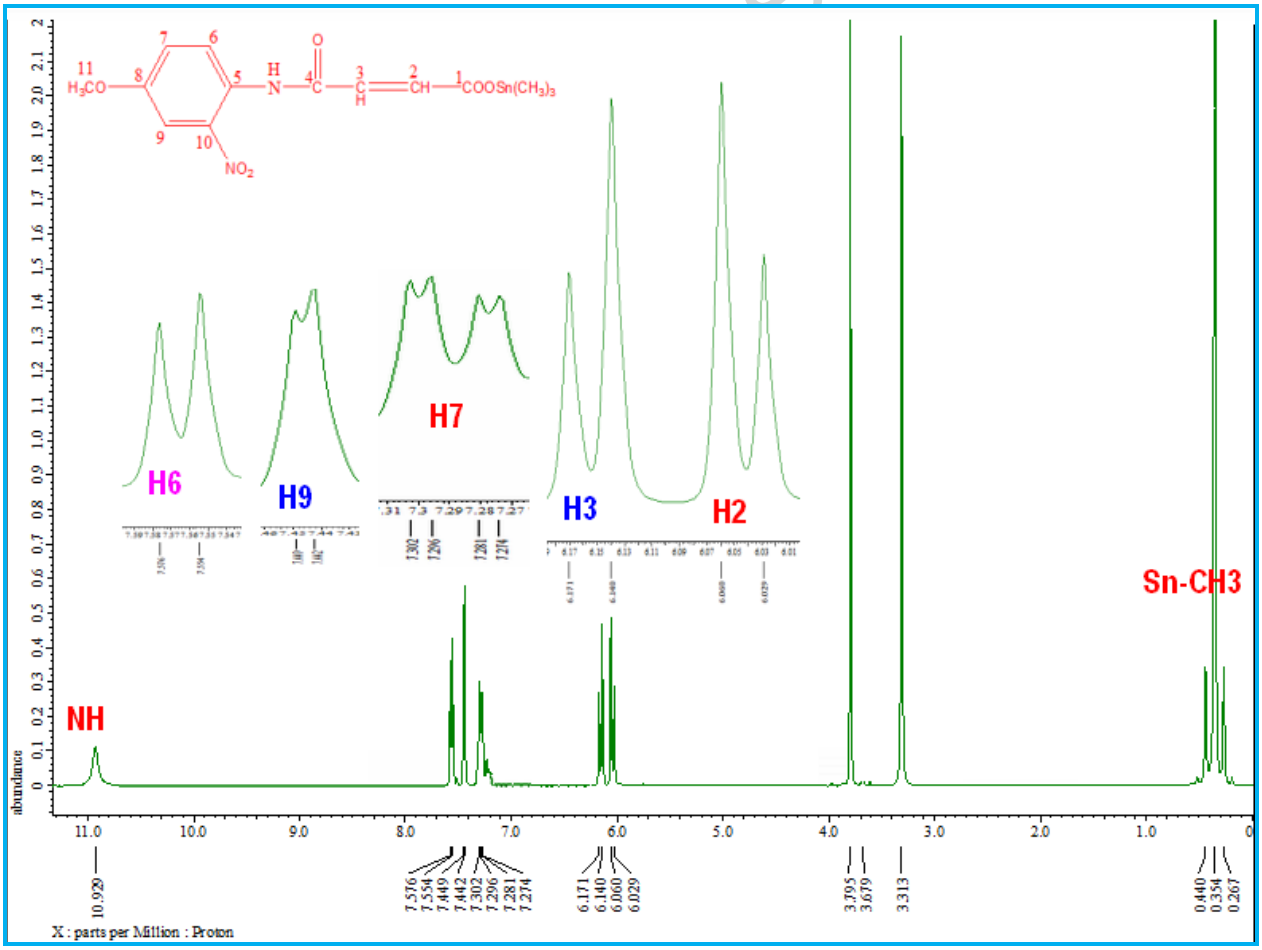

Fig. 1a: ^{1}H NMR spectrum of complex **1**

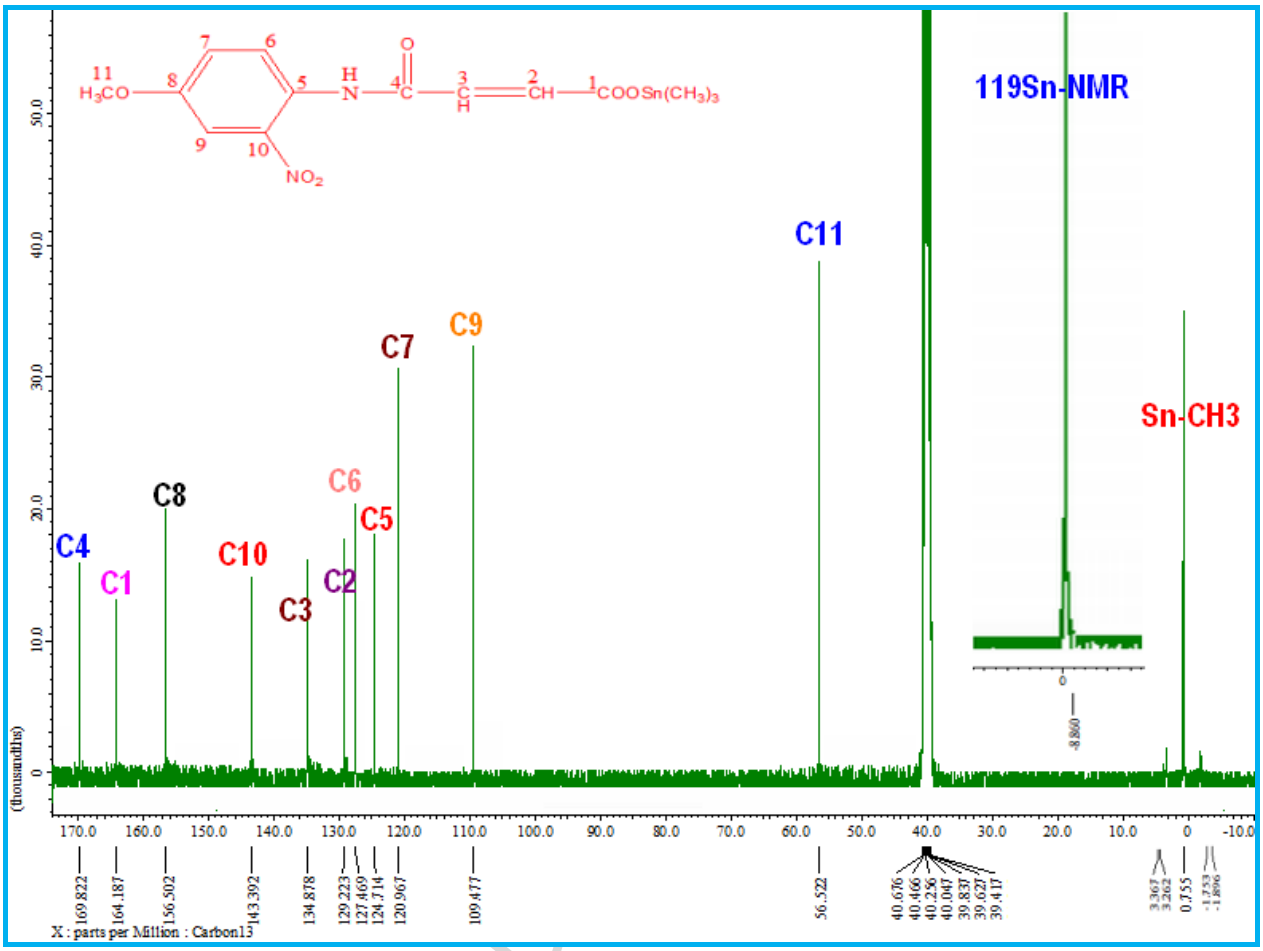

Fig. 1b: ^{13}C and ^{119}Sn NMR spectra of complex **1**

Table 3: ^{1}H NMR data (ppm) for synthesized compounds*

Comp. #	Proton No.												
	OH	**H2**	**H3**	**NH**	**H6**	**H7**	**H9**	**H11**	**α**	**B**	**Γ**	**δ**	**ε**
HL	12.0, s	6.32, d (12)	6.43, d (12)	10.4, s	7.30, d (8.8)	7.51, dd (3.6)	7.45, d (3.6)	3.80, s	-	-	-	-	-
1	-	6.06, d (12.4)	6.17, d (12.4)	10.93, s	7.58, d (8.8)	7.30, dd (2.8)	7.45, d (2.8)	3.82, s	0.35, s [69]	-	-	-	-
2	-	6.12, d (12.4)	6.21, d (12.4)	11.04, s	7.62, d (9.2)	7.30, dd (2.8)	7.45, d (2.8)	3.80, s	1.0, q [76, 64]	1.14, t (8.0)	-	-	-
3	-	6.07, d (12.4)	6.19, d (12.4)	10.71, s	7.66, d (8.8)	7.27, dd (2.8)	7.46, d (2.8)	3.81, s	1.03, t (8.0)	1.51, q	1.23, m	0.80, t (7.2)	-
4	-	6.01, d (12.0)	6.35, d (12.0)	10.69, s	7.50, d (8)	7.24, dd (3.2)	7.45, d (3.2)	3.80, s	-	7.61, d (6.4)	7.10, m	7.53, m	-
5	-	6.13, d (12.4)	6.24, d (12.4)	10.47, s	7.72, d (9.2)	7.29, dd (3.2)	7.47, d (3.2)	3.78, s	1.16, t (8.8)	1.80, m	1.61, m	1.61, m	-
6	-	6.13, d (12.4)	6.25, d (12.4)	11.41, s	7.72, d (8.8)	7.29, dd (2)	7.47, d (2)	3.79, s	0.80, s [100]	-	-	-	-
7	-	6.03, d (12.4)	6.25, d (12.4)	10.71, s	7.52, d (8.8)	7.11, dd (2.8)	7.45, d (2.8)	3.78, s	0.97, t (7.6)	1.50, m	1.30, m	0.81, t (7.6)	-
8	-	6.15, d (12.0)	6.23, d (12.0)	10.14, s	7.51, d (9.2)	7.10, dd (2.8)	7.45, d (2.8)	3.82, s	-	6.97, d (9.2)	7.22, m	7.66, m	-
9	-	6.15, d (12.4)	6.28, d (12.4)	9.98, s	7.53, d (8.4)	7.32, dd (2.8)	7.45, d (2.8)	3.78, s	2.04, s	-	7.59, d (7.6)	7.89, m	7.14, m
10		6.15, d (12.4)	6.32, d (12.4)	10.41, s	7.51, d (9.2)	7.13, dd (2.4)	7.45, d (2.4)	3.80, s	6.97, d (t,9.6),7.32, d (c, 6)	7.24,dd (3.2)	-	-	-
11	-	6.30, d (12.0)	6.37, d (12.0)	10.55, s	7.51, d (8)	7.28, dd (3.2)	7.45, d (3.2)	3.80, s	1.14, t (7.2)	1.55 (bs)	1.38 (bs)	0.80, t (7.2)	-
12	-	6.05, d (12.4)	6.17, d (12.4)	10.99, s	7.57, d (8.8)	7.30, dd (2.8)	7.44, d (2.8)	3.79, s	0.35, s [69]	8.36 {d, 1H (7.6)}, 7.93 (m, 2H), 8.65 {d, 1H, (5.6)} (2,2'-Bipy H)			
13	-	6.06, d (12.4)	6.19, d (12.4)	11.20, s	7.55, d (9.2)	7.32, dd (2.8)	7.43, d (2.8)	3.78, s	0.37, s [70]	9.07 {d, 1H (3.2)}, 7.76 {t, 1H (6.8)}, 8.48 {d, 1H (7.2)}, 7.96 {d, 1H (3.2)} (1,10-phen H)			

* See Schme 1 for compounds numbering. n*J*[119/117Sn-1H] in Hz

Table 4: ^{13}C NMR data (ppm) for synthesized compounds *

Comp. #	Carbon No.																
	C1	**C2**	**C3**	**C4**	**C5**	**C6**	**C7**	**C8**	**C9**	**C10**	**C11**	**α**	β	γ	δ	ε	^{119}Sn
HL	163.8	131.0	131.6	167.4	123.8	128.0	120.7	157.1	109.7	144.2	56.6	-	-	-	-	-	-
1	164.2	129.2	134.9	169.8	124.7	127.5	121.0	156.5	109.5	143.4	56.5	0.8 [516,512]	-	-	-	-	-8.9
2	164.2	130.3	134.1	170.3	124.8	127.3	121.0	156.5	109.5	143.2	56.5	11.1 [491, 470]	10.6 [32]	-	-	-	-18.3
3	164.1	130.5	134.3	170.0	125.0	127.2	120.9	156.4	109.5	142.9	56.5	20.2 [460]	28.2 [28]	26.9 [73]	14.2	-	-6.23
4	163.9	130.7	132.6	169.6	124.4	127.0	120.6	156.2	109.2	143.4	56.3	142.9 [682]	136.4 [46]	128.5 [70]	129. 2	-	-258.3
5	163.5	131.4	133.8	169.3	125.1	126.8	121.1	155.6	109.5	143.5	56.5	37.3 [432, 413]	31.4 [22]	29.2 [73]	27.1	-	-39.6
6	164.2	131.4	133.8	170.2	125.2	126.8	121.1	156.3	109.5	142.7	56.6	-0.7 [833]	-	-	-	-	-189.4
7	163.9	129.6	135.9	169.8	124.6	127.6	121.3	156.6	109.4	142.5	56.0	31.2 [887]	28.0 [44]	26.1 [149]	14.2	-	-208.5
8	164.8	131.5	133.4	170.7	123.5	127.3	121.0	156.8	109.4	143.8	56.3	142.2 [1517]	135.6	128.5	129. 3	-	-247
9	163.6	132.9	135.9	169.8	125.0	127.7	121.3	156.8	109.6	142.5	56.5	19.9	143.0 [189]	135.1	128. 6	12 6. 9	-244.9
10	167.4	131.6	132.8	170.6	123.7	127.7	121.3	156.7	109.7	142.5	56.0	149.7 [616]	129.5	-	-		-271.1
11	163.9	132.9	135.9	169.8	124.2	127.7	121.3	156.8	109.5	142.5	56.5	25.0 29.2	22.6 31.8	33.3 22.8	29.1 14.5		-243.9
12	164.2	129.2	135.0	169.8	124.7	127.5	121.0	156.5	109.5	143.4	56.5	0.8 [527, 504]	149.8,124.6,137.9,120.9,155.7 (2,2-bipy C)				-9.6
13	164.2	129.9	135.2	169.8	124.7	127.5	120.9	156.5	109.5	143.5	56.5	1.3 [517]	150.5,123.9,136.9,129.0,145.9,127.2 (l-1,10-phen C)				-11.1

* See Schme 1 for compounds numbering. n*J*[119/117Sn-13C] in Hz

3.4. X-Ray Crystallography

3.4.1. HL

Figure 2 describes the molecular structure with atom number while Figure 3 describes the 3D-packing diagram with unit cell. Table 6 describes the detailed crystal data while Tables 7 and 8 describe the selected bond lengths and bond angles, respectively. The molecule, (*E*)-4-((4-methoxy-2-nitrophenyl)amino)-4-oxobut-2-enoic acid, crystallizes in orthorhombic system with space group $Pna2_1$. The main plan of the phenyl ring 'C5-C10' and that of maleic acid plan formed by C4-C1/O1-O3 has a dihedral angle of 48.2(3)°. Similarly the plans of phenyl ring and–NHCO 'amide segment' are inclined with an angle of 41.1(3)°. *Anti* conformation was observed for the amide segment NH and carbonyl group. The intramolecular hydrogen bonding, O1-H1···O3, of 2.529Å, results in the formation of 7-membered ring involving C1-C4, O3, H1 and O1 atoms. There are lot of weak intra- and inter-molecular H-bonding such as C3-H3···O2 (3.256Å), C7-H7···O3 (3.528Å), C9-H9···O6 (3.231Å) and C11-H11B···O6 (3.440Å) which are responsible for the formation of flower like 3D packing diagram (Fig. 2b). Table 9 and Figure S1 of the supplementary data presents the detail of intra- and inter-molecular H-bonding present in (*E*)-4-((4-methoxy-2-nitrophenyl)amino)-4-oxobut-2-enoic acid.

Complexes 1 and 2

Figures 4 and 6 describe the molecular structures with atom numbering of complex **1** and **2**, respectively. Table 5 describes the detailed crystal data while Tables 6 and 7 describe the selected bond lengths and bond angles, respectively. Both the molecules crystallize in monoclinic system with space group of $P2_1/c$. A polymeric chain like structures is exhibited by complex **1** and **2** which is formed by ligand, (*E*)-4-((4-methoxy-2-nitrophenyl)amino)-4-oxobut-2-enoic acid. The geometry of complex can be measured form the values of τ (τ = (β-α)/60. Here α is the axial angle and β is the largest basal angle around the tin atom. The values of τ complex **1** and **2** are 0.83 and 0.82, respectively which correspond that the tin atoms are situated in a distorted trigonal bipyramidal geometry [42, 43]. The equatorial plane is made of three R groups (R = CH_3 in complex **1** and C_2H_4 in complex **2**) while the apical positions are occupied by the two oxygen atoms of two (*E*)-4-((4-methoxy-2-nitrophenyl)amino)-4-oxobut-2-enoic acid molecules. The O1-Sn-O2 bond angle is close to a linear arrangement, i.e., 175.69(7)° in complex 1 and 173.50(6)° in complex 2. The sum of the angles subtended at tin atom in the

equatorial position is close to 360°, i.e., 359.7° in complex **1** and 359.6° in complex **2**. The Sn-O bond lengths [Sn1-O1 = 2.323(2)Å & 2.347(1)Å and Sn1-O2 = 2.217(2)Å & 2.227(1)Å] are between the covalent bond length (2.13Å) and van der Waals radii (3.69Å) showing the distorted trigonal bipyramid environment of the tin atom [42, 43]. The value of Sn1-O2 (2.323 Å or 2.327 Å) is slightly greater than the value of normal Sn-O1 (2.054 Å). This may due be presence of weak interaction between O2 and Sn atom making the 5-coordinated geometry. The asymmetric Sn-O separations are also evident from difference in the bond lengths of C1-O1 = 1.265(4) Å, 1.251(2) Å and C1-O2 = 1.253(4) Å, 1.276(2) Å, respectively in complexes **1** and **2** [44]. Here we have got a difference of only 0.012 Å and 0.025 Å, for the complex 1 and 2 which may be due to the chelating nature of (*E*)-4-((4-methoxy-2-nitrophenyl)amino)-4-oxobut-2-enoic acid, and is responsible for the formation of the polymeric structure. Complex **1** exist in wavelike packing diagram which is due the presence of various intra- and inter-molecular interactions within and hydrogen bonding that also stabilize the polymeric chains in zigzag manner which are linked into a three-dimensional network *via* C-H---π interactions. The polar imino hydrogen atom of the amide derivative participates in intramolecular hydrogen bonds (N1-H1---O3). C-H---π, π→π and stacking interactions are responsible for the self-assembled structure of the compounds. Extended networks of O-Sn-O, C-H--O and C-H---π contacts lead to aggregation and a superamolecular assembly. Table 8 gives the detail of all possible intra-and inter-molecular H-bonds.

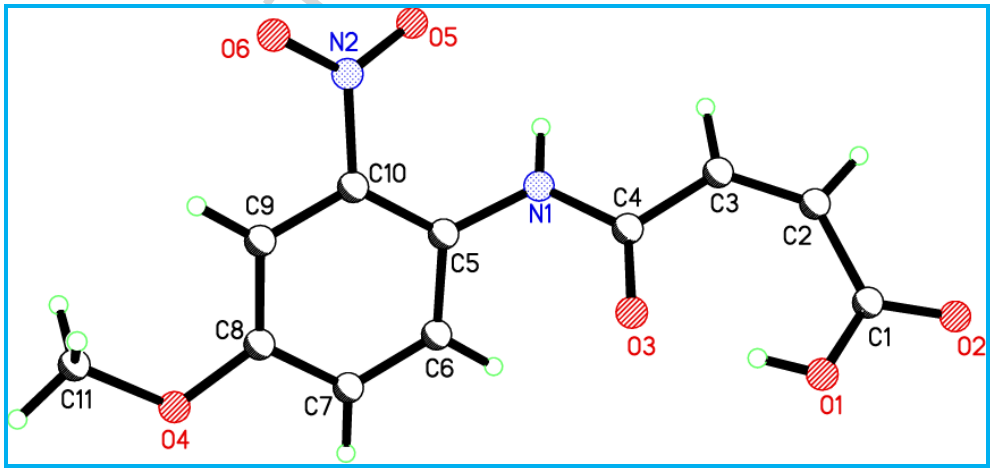

Fig. 2: A perspective view of the (*E*)-4-((4-methoxy-2-nitrophenyl)amino)-4-oxobut-2-enoic acid (HL) with atom number.

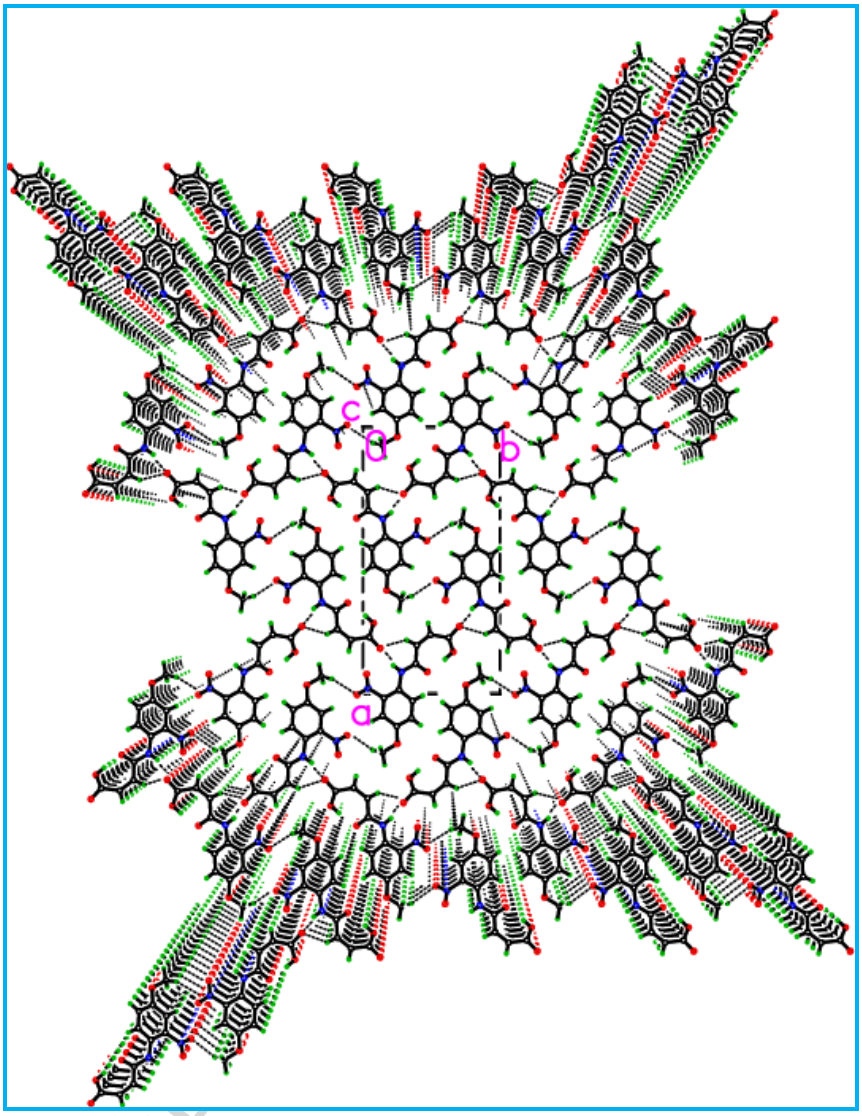

Fig. 3: Packing digram with unit cell of (*E*)-4-((4-methoxy-2-nitrophenyl)amino)-4-oxobut-2-enoic acid (HL).

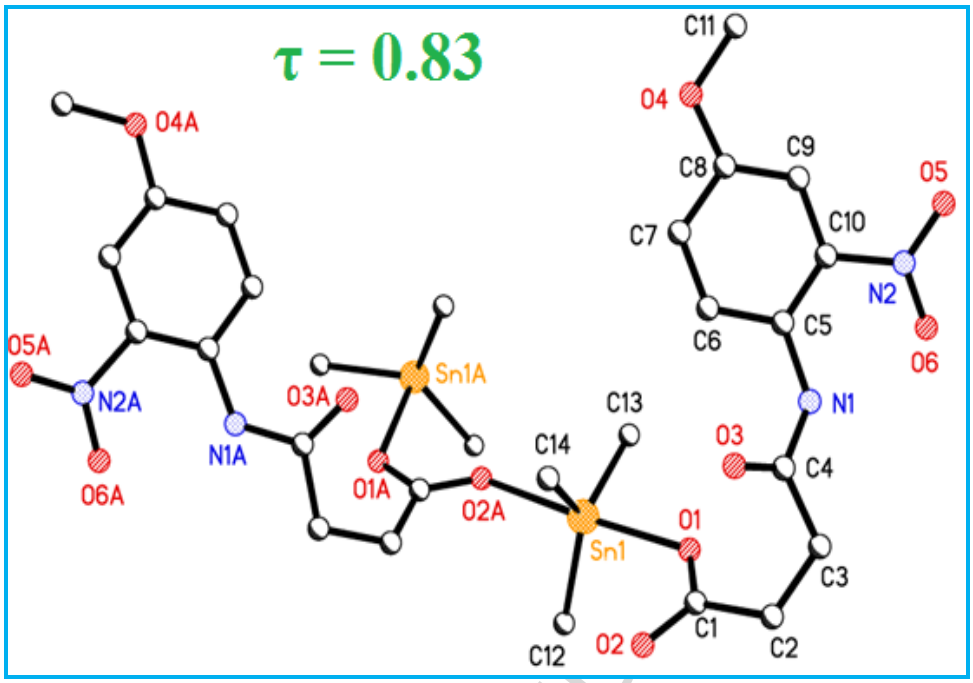

Fig. 4: A perspective view of the complex **1** with atom number.

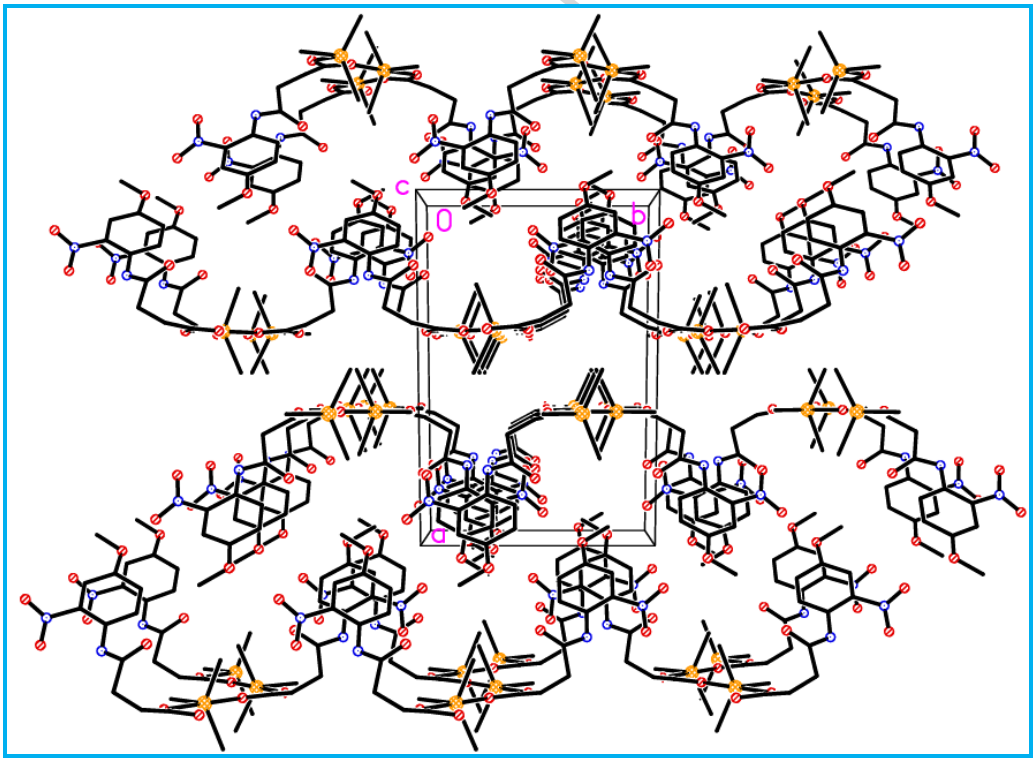

Fig. 5: Packing digram with unit cell of complex **1** viewed along a-axis.

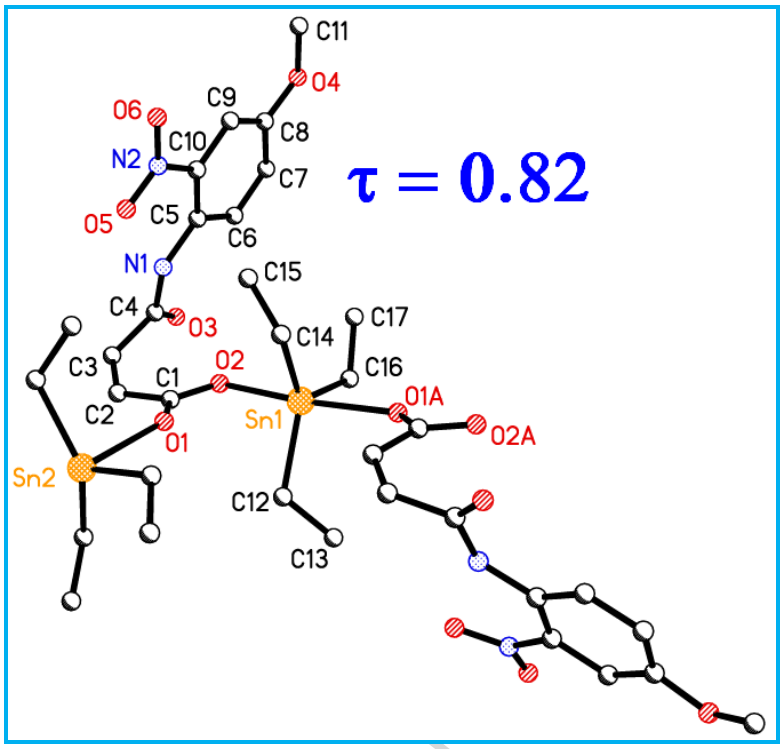

Fig. 6: A perspective view of the complex **2** with atom number.

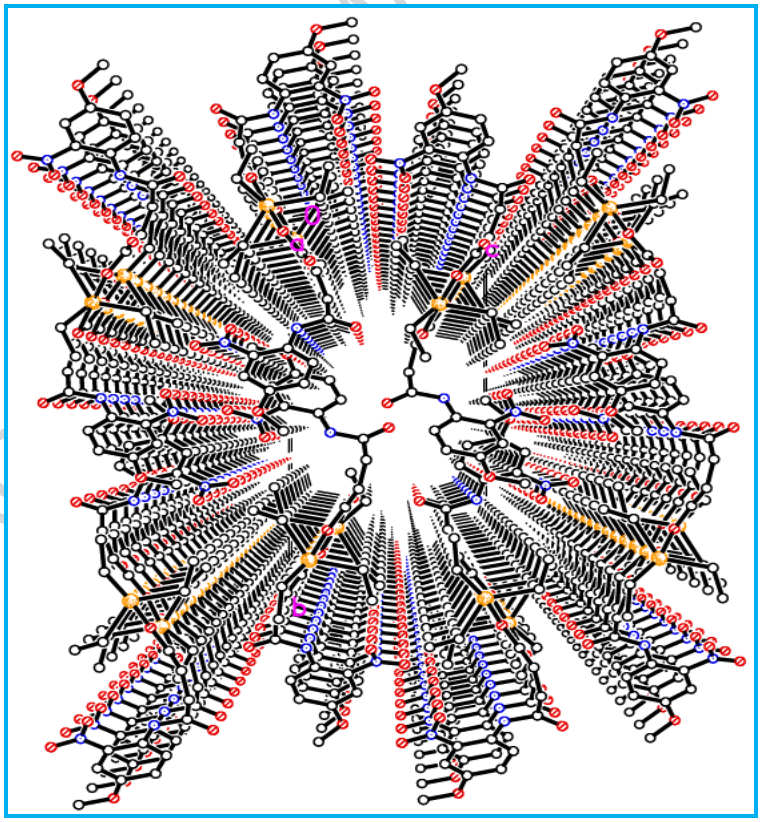

Fig. 7: Packing digram with unit cell of complex **2** viewed along b-axis.

Table 5: Crystal data for HL and complexes 1-2

Parameters	HL	Complex 1	Complex 2
Empirical formula	$C_{11}H_{10}N_2O_6$	$C_{14}H_{18}N_2O_6Sn$	$C_{34}H_{48}N_4O_{12}Sn_2$
Formula weight	266.21	428.99	942.14
T (K)	150(2)	150.15	150(2)
Crystal system	Orthorhombic	Monoclinic	Monoclinic
Space group	$Pna2_1$	$P2_1/c$	$P2_1/c$
a (Å)	23.681(4)	16.440(2)	9.988(3)
b (Å)	12.240(2)	10.7009(13)	28.795(7)
c (Å)	3.7890(7)	9.9748(12)	13.878(4)
α, β, γ (°)	90, 90, 90	90, 104.528(2), 90	90, 101.605(4), 90
V ($Å^3$)	1098.3(3)	1698.7(4)	3909.8(18)
Z	4	4	4
ρ_{calc} (mg/mm^3)	1.610	1.677	1.601
M (mm^{-1})	0.134	1.534	1.341
F(000)	552.0	856.0	1904.0
Crystal size (mm^3)	0.5 × 0.12 × 0.04	0.37 × 0.16 × 0.09	0.41 × 0.11 × 0.07
2θ range for data coll. (°)	6.142 to 54.952	4.586 to 56.662	3.314 to 56.47
Radiation MoKα (λ)	0.71073)	0.71073	0.71073
Reflections collected	5476	17007	39266
Independent reflections	1808 [R_{int} = 0.0324, R_{sigma} = 0.0418]	4223 [R_{int} = 0.0544, R_{sigma} = 0.0500]	9581 [R_{int} = 0.0552, R_{sigma} = 0.0495]
Data/restraints/parameters	1808/1/174	4223/0/211	9581/0/475
S on F^2	1.052	0.960	1.021
Final R indexes [I>=2σ(I)]	R_1 = 0.0360, wR_2 = 0.0830	R_1 = 0.0368, wR_2 = 0.0915	R_1 = 0.0389, wR_2 = 0.0810
CCDC#	997756	997757	997758

Table 6: Selected bond lengths (Å) for HL and complexes 1-2

Bond lengths for HL			
O1-C1	1.309(2)	O2-C1	1.226(2)
C1-C2	1.497(2)	C2-C3	1.388(2)
N1-C4	1.367(2)	N1-C9	1.406(2)
Bond lengths for complex 1			
O1-Sn1	2.323(2)	C12-Sn1	2.125(3)
O2-Sn1	2.217(2)	C13-Sn1	2.125(3)
C1-C2	1.522(3)	C14-Sn1	2.122(3)
C1-O1	1.265(4)	C1-O2	1.253(4)
Bond lengths for complex 2			
O1-Sn1	2.347(1)	C12-Sn1	2.140(3)
O2-Sn1	2.227(1)	C14-Sn1	2.138(3)
C1-C2	1.514(3)	C16-Sn1	2.136(2)
C1-O1	1.251(2)	C1-O2	1.276(2)

Table 7: Selected bond angles (˚) for HL and complexes 1-2

Bond angles for HL			
O1-C1-O2	120.6(2)	O2-C1-C2	118.5(3)
O1-C1-C2	120.8(2)	C1-C2-C3	132.5(3)
N1-C4-C3	114.2(2)	C4-N1-C5	122.6(2)
Bond angles for complex 1			
O1-Sn1-C12	87.4(1)	C12-Sn1-O2	93.94(9)
O1-Sn1-C13	86.9(1)	C13-Sn1-O2	88.9(1)
O1-Sn1-C14	90.4(1)	C14-Sn1-O2	92.08(9)
O1-Sn1-O2	175.69(7)	C12-Sn1-C13	118.0(1)
O1-C1-O2	122.3(2)	C12-Sn1-C14	126.0(1)
O1-C1-C2	120.8(2)	C13-Sn1-C14	115.7(1)
Bond angles for complex 2			
O1-Sn1-C12	87.71(8)	C12-Sn1-O2	94.34(9)
O1-Sn1-C14	89.68(9)	C14-Sn1-O2	94.21(9)
O1-Sn1-C16	86.01(8)	C16-Sn1-O2	87.64(8)
O1-Sn1-O2	173.50(6)	C12-Sn1-C14	124.5(1)
O1-C1-O2	122.6(2)	C12-Sn1-C16	120.6(1)
O1-C1-C2	120.9(2)	C14-Sn1-C16	114.5(1)

Table 8: Hydrogen-bond angles and bond lengths for HL and complexes 1-2

D-H····A	**D-H** (Å)	**H····A** (Å)	**D····A** (Å)	**D-H····A** (˚)
		HL		
O1-H1···O3	0.84	1.69	2.529(2)	173.9
C3-H3···O2[1]	0.95	2.46	3.256(4)	140.9
N1-H1A···O2[1]	0.88	2.09	2.935(3)	161.3
N1-H1A···O5	0.88	2.26	2.723(3)	113.0
C7-H7···O3[2]	0.95	2.65	3.528(3)	154.5
C9-H9···O6[3]	0.95	2.60	3.231(3)	124.1
C11-H11B···O6[3]	0.98	2.51	3.440(4)	158.0
		Complex 1		
N1-H1···O6	0.880	2.055	122.72	2.637
C6-H6···O3	0.950	2.372	113.32	2.883
		Complex 2		
C2-H2···O3A[i]	0.95	2.53	3.155(4)	123.8
N1-H1···O5	0.88	1.94	2.624(5)	133.3
C6-H6···O3	0.95	2.23	2.866(5)	123.1
N1A-H1A···O5A	0.88	1.94	2.624(4)	133.5
C6A-H6A···O3A	0.95	2.23	2.877(5)	124.3
C11A-H11DA···O6A[ii]	0.98	2.48	3.294(5)	140.4

Symmetry transformations used to generate equivalent atoms for **HL:** 1)-1/2-X,-1/2+Y,-1/2+Z; 2) -X,1-Y,-1/2+Z; 3) -X,-Y,-1/2+Z

Symmetry transformations used to generate equivalent atoms for complex **2** (i) -1+X,1/2-Y,-1/2+Z; (ii) 4-X,-Y,1-Z

3.4. Mass Spectrometry

The MS data of the ligand and its complexes determined by ESI method is presented in Table 9. Scheme 2 shows the detail fragmentation pattern of ligand, (*E*)-4-((4-methoxy-2-nitrophenyl)amino)-4-oxobut-2-enoic acid (HL). Both $[M]^+$ and $[M+1]^+$ were appeared in the MS of the HL with $[M+1]^+$ as base peak at m/z = 269.

In the MS of the synthesized organotin carboxylates (**1-13**), the low intensity M^+ (molecular ion peaks) and $[MNa]^+$ are observed in all spectra. Triorganotin compounds undergo fragmentation by three pathways based on observed m/z in their spectra. In one pathway various fragments

such as COOR' and R on elimination gave $[Sn]^+$ as end product. The other two pathways after primary elimination of $[R]^+$ and $[R_3Sn]^+$ groups and then elimination of COO and successive R (in one of the pathway) results in the formation of $[R']^+$, which shows similar pattern for the further elimination of different groups (Supplementary data; Scheme S1).

A bit different scheme of mass fragmentation pattern has been suggested for the diorganotin compounds (Supplementary data; Scheme S2) but these pathways end up in similar manner as suggested for the triorganotin compounds. In addition, the following ions: $[C_4H_9]^+$, $[C_6H_5]^+$, $[C_7H_7]^+$ and $[C_8H_{17}]^+$ are also observed with reasonable intensities in the mass spectra of all organotin(IV) derivatives.

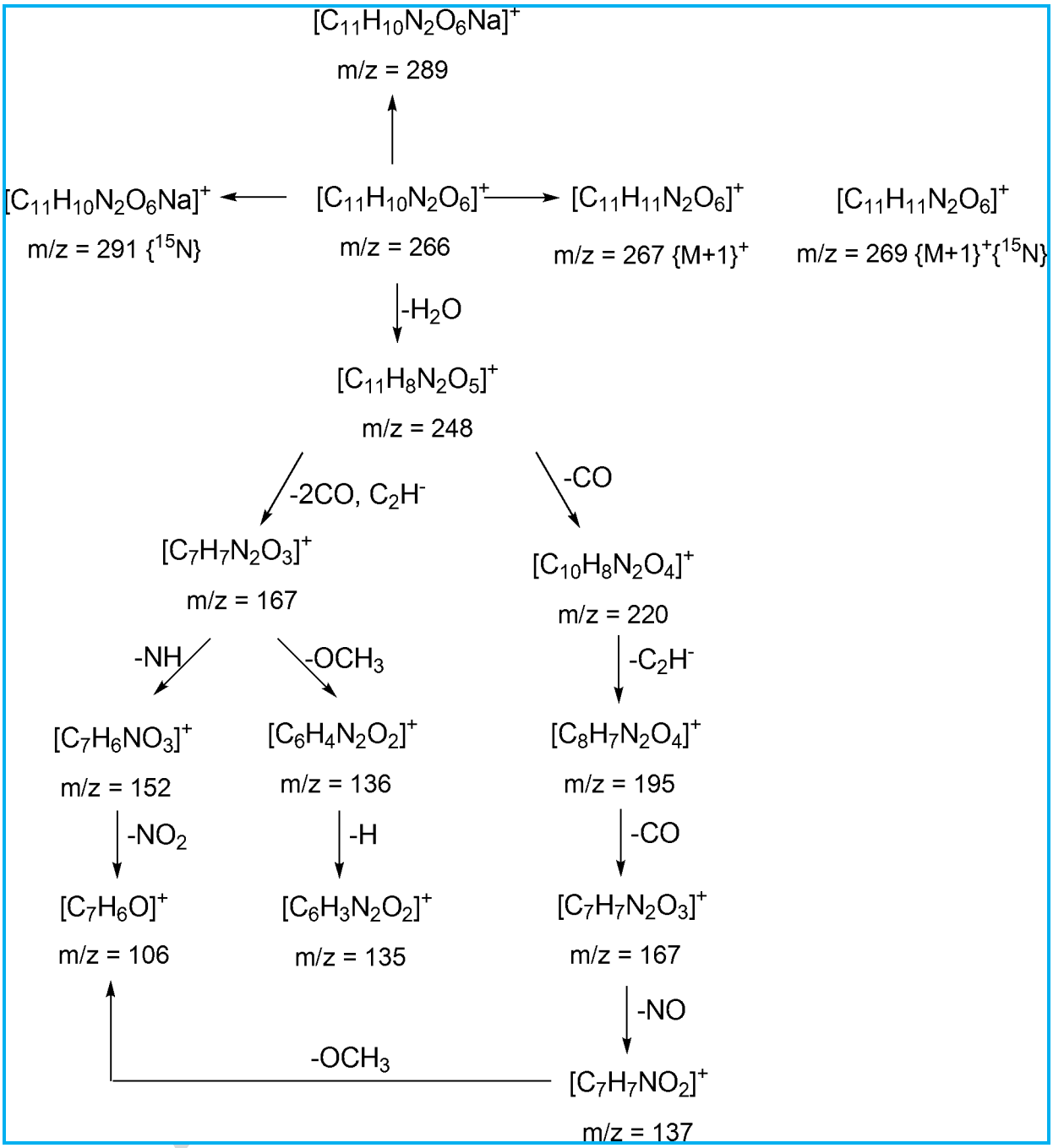

Scheme 2: General mass fragmentation pattern for HL

Table 9: ESI-Mass fragmentation data with m/z value of the synthesized compounds*

Comp. No	Fragment with m/z (%)
HL	$[C_{11}H_{10}N_2O_6Na]^+$ = 289 (90); $[C_{11}H_{10}N_2O_6Na]^+$ = 291 (100); $[C_{11}H_{10}N_2O_6]^+$ = 266 (10); $[C_{11}H_{11}N_2O_6]^+$, $\{M+1\}^+$ = 267 (95); $[C_{11}H_{11}N_2O_6]^+$ = 269 (50); $[C_{11}H_8O_5N_2]^+$ = 248 (23); $[C_{10}H_8N_2O_4]^+$ = 220 (5); $[C_8H_7N_2O_4]^+$ = 195 (30); $[C_7H_7N_2O_3]^+$ = 167 (10); $[C_7H_7NO_2]^+$ = 137 (5); $[C_7H_6O]^+$ = 106 (11); $[C_7H_6NO_3]^+$ = 152 (12); $[C_6H_4N_2O_2]^+$ = 136 (15); $[C_6H_3N_2O_2]^+$ = 135 (11)
1	$[C_{14}H_{18}N_2O_6SnNa]^+$ = 453 (23); $[C_{14}H_{18}N_2O_6Sn]^+$ = 430 (39); $[C_{11}H_9O_6N_2]^+$ = 265 (13); $[C_{10}H_9N_2O_4]^+$ = 221 (26); $[C_3H_9Sn]^+$ = 165 (100); $[C_2H_6Sn]^+$ = 150 (6); $[CH_3Sn]^+$ = 135 (9); $[Sn]^+$ = 120 (6); $[C_{13}H_{15}N_2O_6Sn]^+$ = 415 (9); $[C_{12}H_{15}N_2O_4Sn]^+$ = 371 (9); $[C_{11}H_{12}N_2O_4Sn]^+$ = 356 (1); $[C_{10}H_9N_2O_4Sn]^+$ = 341 (9)
2	$[C_{17}H_{24}N_2O_6SnNa]^+$ = 493 (5); $[C_{17}H_{24}N_2O_6Sn]^+$ = 430 (8); $[C_{11}H_9N_2O_6]^+$ = 265 (13); $[C_{10}H_9N_2O_4]^+$ = 221 (86); $[C_6H_{15}Sn]^+$ = 207 (100); $[C_4H_{10}Sn]^+$ = 178 (11); $[C_2H_5Sn]^+$ = 149 (10); $[Sn]^+$ = 120 (11); $[C_{15}H_{19}N_2O_6Sn]^+$ = 443 (1); $[C_{14}H_{19}N_2O_4Sn]^+$ = 399 (1); $[C_{12}H_{14}N_2O_4Sn]^+$ = 370 (2); $[C_{12}H_{14}N_2O_4]^+$ = 250 (1)
3	$[C_{23}H_{36}N_2O_6SnNa]^+$ = 579 (34); $[C_{23}H_{36}N_2O_6Sn]^+$ = 556 (32); $[C_{11}H_9N_2O_6]^+$ = 265 (12); $[C_{10}H_9N_2O_4]^+$ = 221 (10); $[C_{12}H_{27}Sn]^+$ = 291 (100); $[C_8H_{18}Sn]^+$ = 234 (11); $[C_4H_9Sn]^+$ = 177 (9); $[Sn]^+$ = 120 (7); $[C_{19}H_{27}N_2O_6Sn]^+$ = 499 (29); $[C_{18}H_{27}N_2O_4Sn]^+$ = 455 (34); $[C_{14}H_{18}N_2O_4Sn]^+$ = 398 (45); $[C_{14}H_{18}N_2O_4Sn]^+$ = 341 (41)
4	$[C_{29}H_{24}N_2O_6SnNa]^+$ = 639 (17); $[C_{29}H_{24}N_2O_6Sn]^+$ = 616 (7); $[C_{11}H_9N_2O_6]^+$ = 265 (2); $[C_{10}H_9N_2O_4]^+$ = 221 (2); $[C_{18}H_{15}Sn]^+$ = 351 (100); $[C_{12}H_{10}Sn]^+$ = 274 (17); $[C_4H_9Sn]^+$ = 197 (23); $[Sn]^+$ = 120 (1); $[C_{23}H_{19}N_2O_6Sn]^+$ = 539 (15); $[C_{22}H_{19}N_2O_4Sn]^+$ = 495 (34); $[C_{16}H_{14}N_2O_4Sn]^+$ = 418 (16); $[C_{10}H_9N_2O_4Sn]^+$ = 341 (41)
5	$[C_{29}H_{42}N_2O_6SnNa]^+$ = 657 (11); $[C_{29}H_{42}N_2O_6Sn]^+$ = 634 (3); $[C_{11}H_9N_2O_6]^+$ = 265 (25); $[C_{10}H_9N_2O_4]^+$ = 221 (29); $[C_{18}H_{33}Sn]^+$ = 369 (100); $[C_{12}H_{22}Sn]^+$ = 287 (30); $[C_6H_{11}Sn]^+$ = 197 (7); $[Sn]^+$ = 120 (12); $[C_{23}H_{31}N_2O_6Sn]^+$ = 551 (28); $[C_{22}H_{31}N_2O_4Sn]^+$ = 507 (34); $[C_{16}H_{20}N_2O_4Sn]^+$ = 424 (3); $[C_{10}H_9N_2O_4Sn]^+$ = 341 (11)

6	$[C_{24}H_{24}N_4O_{12}SnNa]^+$, m/z = 703 (30); $[C_{24}H_{24}N_4O_{12}Sn]^+$, m/z = 680 (11); $[C_{23}H_{21}N_4O_{12}Sn]^+$, m/z = 665 (10); $[C_{12}H_{12}N_2O_6Sn]^+$ = 400 (9); $[C_{11}H_9N_2O_6Sn]^+$ = 385 (3); $[C_{11}H_9N_2O_6]^+$ = 265 (14); $[C_{10}H_9N_2O_4]^+$ = 221 (29); $[C_2H_6Sn]^+$ = 150 (14); $[CH_3Sn]^+$ = 135 (13); $[Sn]^+$ = 120 (12); $[C_{13}H_{15}N_2O_6Sn]^+$ = 415 (100); $[C_{12}H_{15}N_2O_4Sn]^+$ = 371 (43); $[C_{11}H_{12}N_2O_4Sn]^+$ = 356 (35); $[C_{10}H_9N_2O_4Sn]^+$ = 341 (15); $[C_{22}H_{21}N_4O_{10}Sn]^+$ = 621 (2)
7	$[C_{30}H_{36}N_4O_{12}SnNa]^+$ = 787 (11); $[C_{30}H_{36}N_4O_{12}Sn]^+$ = 764 (2); $[C_{26}H_{27}N_4O_{12}Sn]^+$ = 707 (3); $[C_{15}H_{18}N_2O_6Sn]^+$ = 442 (6); $[C_{11}H_9N_2O_6Sn]^+$ = 385 (2); $[C_{11}H_9N_2O_6]^+$ = 265 (7); $[C_{10}H_9N_2O_4]^+$ = 221 (12); $[C_8H_{18}Sn]^+$ = 234 (23); $[C_4H_9Sn]^+$ = 177 (100); $[Sn]^+$ = 120 (20); $[C_{19}H_{27}N_2O_6Sn]^+$ = 499 (43); $[C_{18}H_{27}N_2O_4Sn]^+$ = 455 (27); $[C_{14}H_{18}N_2O_4Sn]^+$ = 398 (21); $[C_{10}H_9N_2O_4Sn]^+$ = 341 (21); $[C_{25}H_{27}N_4O_{10}Sn]^+$ = 663 (2)
8	$[C_{34}H_{28}N_4O_{12}SnNa]^+$ = 827 (10); $[C_{34}H_{28}N_4O_{12}Sn]^+$ = 804 (5); $[C_{28}H_{23}N_4O_{12}Sn]^+$ = 727 (33); $[C_{17}H_{14}N_2O_6Sn]^+$ = 462 (23); $[C_{11}H_9N_2O_6Sn]^+$ = 385 (31); $[C_{11}H_9N_2O_6]^+$ = 265 (43); $[C_{10}H_9N_2O_4]^+$ = 221 (46); $[C_{12}H_{10}Sn]^+$ = 274 (20); $[C_6H_5Sn]^+$ = 197 (65); $[Sn]^+$ = 120 (31); $[C_{23}H_{19}N_2O_6Sn]^+$ = 539 (100); $[C_{22}H_{19}N_2O_4Sn]^+$ = 495 (50); $[C_{16}H_{14}N_2O_4Sn]^+$ = 418 (20); $[C_{10}H_9N_2O_4Sn]^+$ = 341 (12); $[C_{27}H_{25}N_4O_{10}Sn]^+$ = 685 (9)
9	$[C_{37}H_{35}N_4O_{12}SnNa]^+$ = 870 (12); $[C_{37}H_{35}N_4O_{12}Sn]^+$ = 847 (5); $[C_{30}H_{28}N_4O_{12}Sn]^+$ = 756 (33); $[C_{17}H_{14}N_2O_6Sn]^+$ = 491 (21); $[C_{11}H_7N_2O_6Sn]^+$ = 400 (34); $[C_{11}H_9N_2O_6]^+$ = 265 (33); $[C_{10}H_9N_2O_4]^+$ = 221 (46); $[C_{14}H_{14}Sn]^+$ = 302 (9); $[C_7H_7Sn]^+$ = 211 (65); $[Sn]^+$ = 120 (31); $[C_{26}H_{26}N_2O_6Sn]^+$ = 582 (100); $[C_{19}H_{19}N_2O_6Sn]^+$ = 491 (46); $[C_{18}H_{19}N_2O_4Sn]^+$ = 447 (34); $[C_{11}H_{12}N_2O_4Sn]^+$ = 356 (21); $[C_{29}H_{28}N_4O_{10}Sn]^+$ = 712 (12)
10	$[C_{26}H_{24}N_4O_{12}SnNa]^+$ = 727 (23); $[C_{26}H_{24}N_4O_{12}Sn]^+$ = 704 (10); $[C_{24}H_{21}N_4O_{12}Sn]^+$ = 677 (4); $[C_{13}H_{12}N_2O_6Sn]^+$ = 412 (3); $[C_{11}H_9N_2O_6Sn]^+$ = 385 (2); $[C_{11}H_9N_2O_6]^+$ = 265 (2); $[C_{10}H_9N_2O_4]^+$ = 221 (29); $[C_4H_6Sn]^+$ = 174 (3); $[C_2H_3Sn]^+$ = 147 (3); $[Sn]^+$ = 120 (3); $[C_{15}H_{15}N_2O_6Sn]^+$ = 439 (100); $[C_{14}H_{15}N_2O_4Sn]^+$ = 395 (3); $[C_{12}H_{12}N_2O_4Sn]^+$ = 368 (5); $[C_{10}H_9N_2O_4Sn]^+$ = 341 (25); $[C_{23}H_{21}N_4O_{10}Sn]^+$ = 633 (5)
11	$[C_{38}H_{52}N_4O_{12}SnNa]^+$ = 899 (43); $[C_{38}H_{52}N_4O_{12}Sn]^+$ = 876 (60); $[C_{30}H_{35}N_4O_{12}Sn]^+$ = 763 (6); $[C_{19}H_{24}N_2O_6Sn]^+$ = 496

	(11); $[C_{11}H_7N_2O_6Sn]^+$ = 383 (22); $[C_{11}H_9N_2O_6]^+$ = 265 (100); $[C_{10}H_9N_2O_4]^+$ = 221 (13); $[C_{16}H_{34}Sn]^+$ = 346 (9); $[C_8H_{17}Sn]^+$ = 233 (12); $[Sn]^+$ = 120 (5); $[C_{27}H_{41}N_2O_6Sn]^+$ = 609 (80); $[C_{26}H_{41}N_2O_4Sn]^+$ = 565 (4); $[C_{18}H_{24}N_2O_4Sn]^+$ = 452 (8); $[C_{10}H_7N_2O_4Sn]^+$ = 339 (18); $[C_{29}H_{35}N_4O_{10}Sn]^+$ = 719 (5)
12	$[C_{24}H_{26}N_4O_6SnNa]^+$ = 609 (11); $[C_{24}H_{26}N_4O_6Sn]^+$ = 586 (5); $[C_{14}H_{18}N_2O_6Sn]^+$ = 430 (12); $[C_{11}H_9O_6N_2]^+$ = 265 (100); $[C_{10}H_9N_2O_4]^+$ = 221 (22); $[C_3H_9Sn]^+$ = 165 (43); $[C_2H_6Sn]^+$ = 150 (31); $[CH_3Sn]^+$ = 135 (50); $[Sn]^+$ = 120 (14); $[C_{23}H_{23}N_4O_6Sn]^+$ = 571 (15); $[C_{22}H_{23}N_4O_4Sn]^+$ = 527 (12); $[C_{21}H_{20}N_4O_4Sn]^+$ = 512 (5); $[C_{11}H_{12}N_2O_4Sn]^+$ = 356 (2); $[C_{10}H_{12}N_2O_2Sn]^+$ = 312 (57); $[C_9H_{12}N_2O_2]^+$ = 177 (25); $[C_8H_9N_2O_2]^+$ = 162 (33); $[C_{10}H_8N_2]^+$ = 156 (5); $[C_{10}H_9N_2]^+$ = 157 (34)
13	$[C_{26}H_{26}N_4O_6SnNa]^+$ = 633 (2); $[C_{26}H_{26}N_4O_6Sn]^+$ = 610 (3); $[C_{14}H_{18}N_2O_6Sn]^+$ = 430 (21); $[C_{11}H_9O_6N_2]^+$ = 265 (100); $[C_{10}H_9N_2O_4]^+$ = 221 (4); $[C_3H_9Sn]^+$ = 165 (24); $[C_2H_6Sn]^+$ = 150 (5); $[CH_3Sn]^+$ = 135 (11); $[Sn]^+$ = 120 (2); $[C_{25}H_{23}N_4O_6Sn]^+$ = 595 (12); $[C_{24}H_{23}N_4O_4Sn]^+$ = 551 (5); $[C_{23}H_{20}N_4O_4Sn]^+$ = 536 (13); $[C_{11}H_{12}N_2O_4Sn]^+$ = 356 (22); $[C_{10}H_{12}N_2O_2Sn]^+$ = 312 (12); $[C_{10}H_{12}N_2O_2]^+$ = 192 (21); $[C_9H_9N_2O_2]^+$ = 177 (54); $[C_{12}H_8N_2]^+$ = 180 (7)

* See Schme 1 for compounds numbering.

3.5. DNA binding study

UV-visible absorption spectroscopic technique was used for the evaluation of interaction between the SS-DNA and the synthesized compounds. Figures 8-10 demonstrate the UV-visible spectra of (*E*)-4-((4-methoxy-2-nitrophenyl)amino)-4-oxobut-2-enoic acid (**HL**), compounds **2** and **4** with different concentrations of DNA (for Compounds **5** and **10** see supplementary data: Figures S2 and S3). A strong absorption peak in the range of 351-444 nm was exhibited by the screened compounds. This peak is mainly due to the π-π* transition of the aromatic ring of the interacting compound and nitrogenous DNA bases [21]. The binding of the compound with DNA causes change in absorption as well as in wavelength. If the compound binds to DNA through intercalative mode then a red shift in wavelength (usually consistent with the strength of the intercalative interaction) along with hyprochromic shift (because of strong stacking interaction between nitrogenous DNA bases and aromatic chromophore of the compound) occur [15].

Based on the above viewpoint the intercalative mode of binding is suggested for the interaction between the screened compound and DNA as both red shift in wavelength (about 3-5 nm) and obvious hypochromic shift were observed [45]. The binding constant was determined from the ratio of the intercept-to-slope of $A_o/(A-A_o)$ *vs.* 1/[DNA] plot in Benesi-Hildebrand's equation [46]. $\Delta G = -RT \ln K$ was used for the determination of Gibb's free energy. The values of *K* and ΔG are given in Table 10. The order of interaction with DNA is as: **5** > **4** > **2** > **HL**.

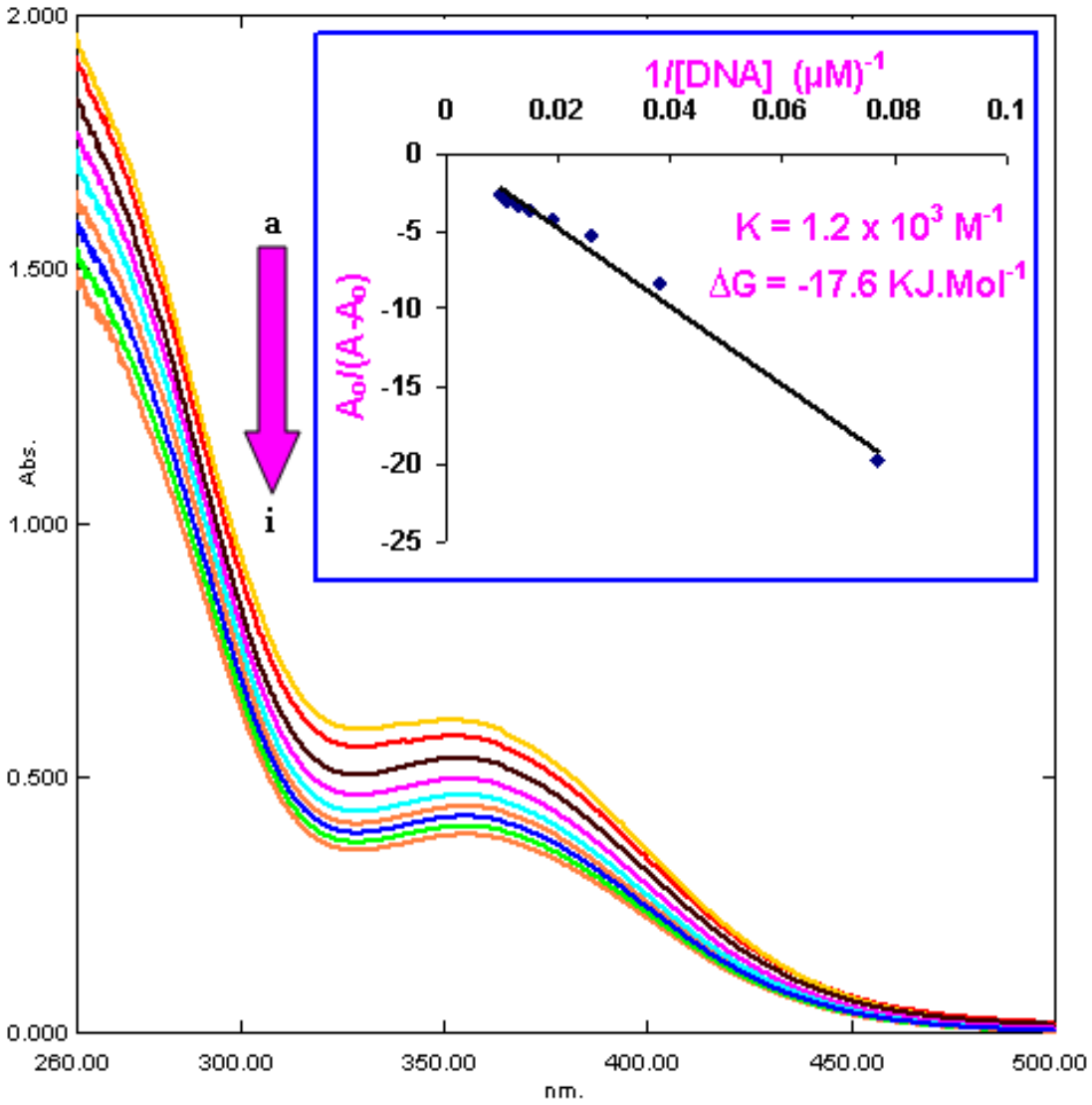

Fig. 8: Absorption spectrum of 1 mM **HL** in the absence (a) and presence of 9 (b), 18 (c), 27 (d), 36 (e), 45 (f), 54 (g), 63 (h) and 72 (i) μM DNA. The arrow indicates the increasing conc. of DNA. The inset graph represents the values of K and ΔG.

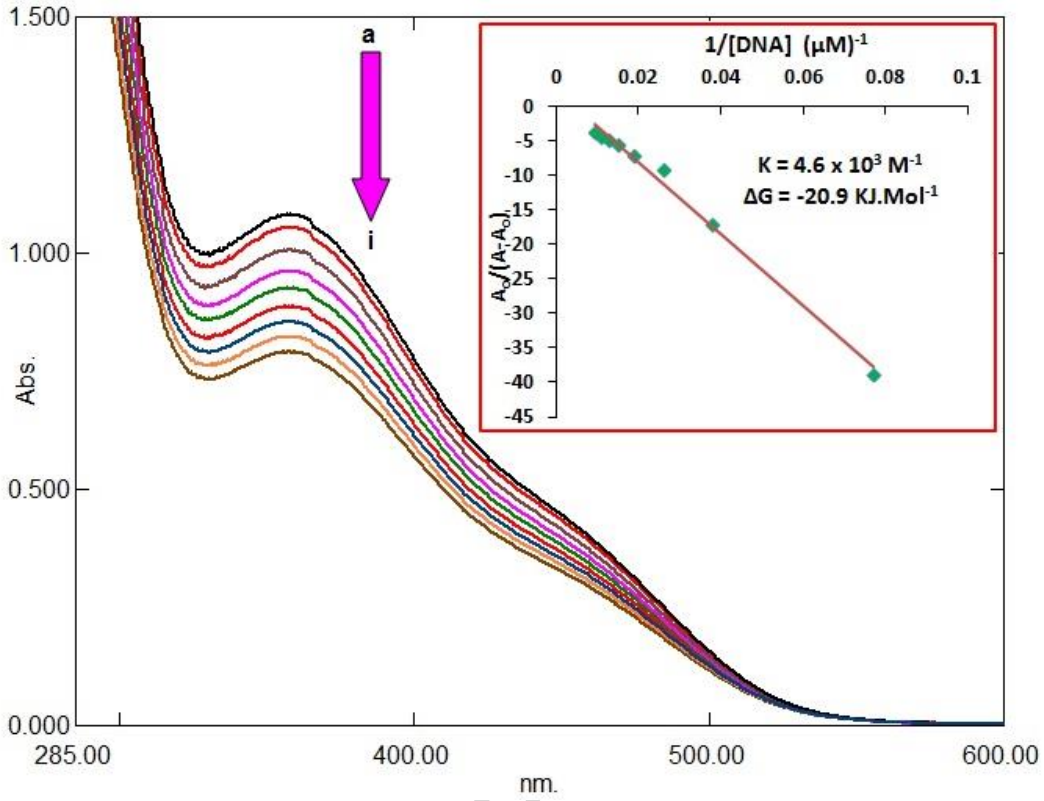

Fig. 9: Absorption spectrum of 1 mM complex **2** in the absence (a) and presence of 9 (b), 18 (c), 27 (d), 36 (e), 45 (f), 54 (g), 63 (h) and 72 (i) μM DNA. The arrow indicates the increasing conc. of DNA. The inset graph represents the values of K and ΔG.

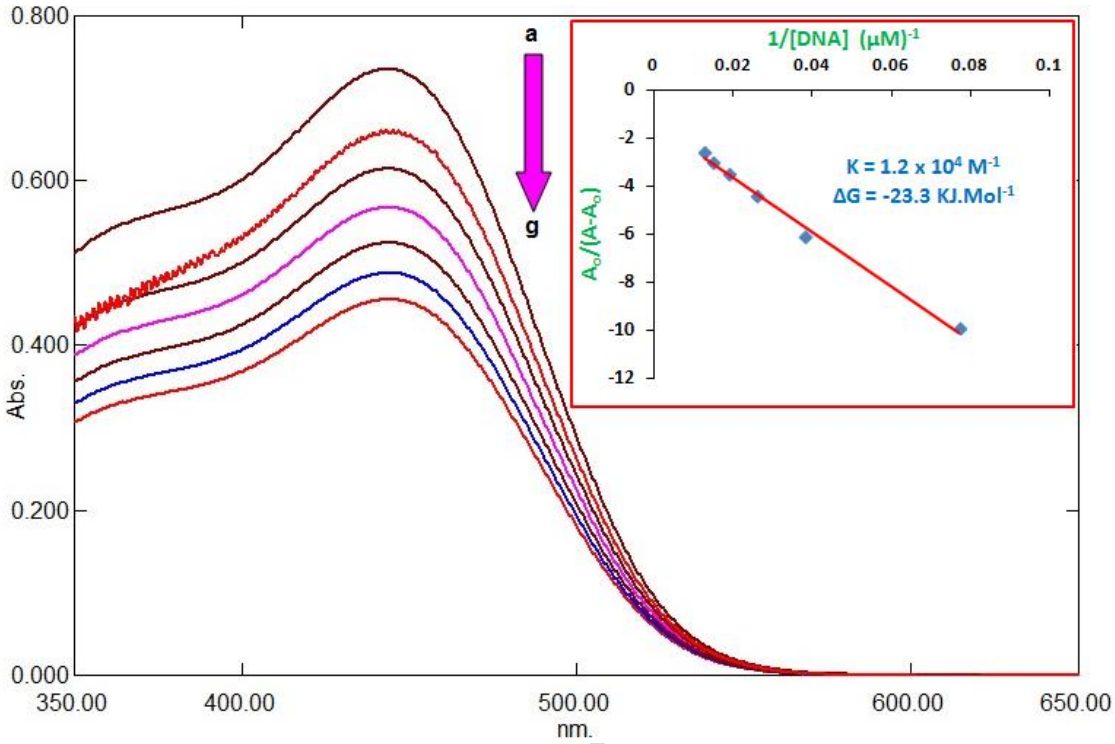

Fig. 10: Spectrum of 1 mM complex **4** in the absence (a) and presence of 9 (b), 18 (c), 27 (d), 36 (e), 45 (f) and 54 (g) µM DNA. The arrow indicates the increasing conc. of DNA. The inset graph represents the values of K and ΔG.

Table 10: Binding constant and Gibb's free energy values for the selected compounds*

Compound No.	K (M^{-1})	ΔG ($KJ.Mol^{-1}$)
HL	1.2×10^3	-17.6
2	4.6×10^3	-20.9
4	7.57×10^3	-22.2
5	1.2×10^4	-23.3
10	2.3×10^3	-19.1

* See Schme 1 for compounds numbering.

3.6. Anticancer Activity

Table 11 presents the anticancer activity data of the evaluated compounds. Those compounds which have the ability of eliminating cancer affected cells without affecting the normal cells have therapeutic edge for cancer treatment [47]. Cytotoxicity evaluation of the investigated compounds explored another biological feature of the synthesized compounds as being strong

anticancer agents. The data clearly demonstrate that the tested compounds have dose dependent effect on the growth and proliferation of H-157 and BHK-21 cell lines. Compounds **6**, **10** and **12** have shown maximum activity. The results revealed that all the tested compounds showed good cytotoxicity against H-157 and BHK-21 cell lines in a dose dependent manner. Overall the evaluated compounds have shown good cytotoxic effect at different concentrations.

Table 11: Anticancer activity of the synthesized compounds[a]

Comp. No	Cytotoxicity (%) against BHK-21				Cytotoxicity (%) against H-157			
	Dose Conc. (µM)				Dose Conc. (µM)			
	100	10	1	0.1	100	10	1	0.1
HL	47.1 ± 1.3	44.3 ± 1.2	40.9 ± 1.1	33.2 ± 1.2	67.4 ± 2.5	64.3 ± 1.5	56.6 ± 2.8	50.6 ± 2.5
NaL	51.5 ± 2.4	45.7 ± 1.3	42.9 ± 2.4	39.6 ± 1.3	58.7 ± 2.1	55.4 ± 1.3	51.1 ± 2.3	46.5 ± 2.3
1	51.9 ± 1.5	47.6 ± 2.2	44.1 ± 2.9	40.8 ± 1.5	42.6 ± 2.6	33.4 ± 1.4	27.1 ± 1.5	17.8 ± 1.5
2	49.6 ± 1.4	43.3 ± 1.1	38.4 ± 0.3	33.2 ± 1.5	48.2 ± 2.3	44.1 ± 3.2	40.9 ± 1.7	32.5 ± 2.1
3	52.9 ± 1.3	50.7 ± 1.5	47.3 ± 2.3	45.1 ± 1.8	51.0 ± 1.3	44.2 ± 2.5	38.1 ± 2.4	32.8 ± 1.3
4	39.8 ± 3.2	34.3 ± 2.1	30.5 ± 1.1	28.9 ± 1.7	37.1 ± 1.6	29.3 ± 1.3	26.6 ± 1.3	22.1 ± 1.7
5	57.2 ± 1.6	55.8 ± 3.5	51.2 ± 1.4	48.3 ± 1.1	66.5 ± 1.5	57.4 ± 2.7	52.7 ± 1.1	47.9 ± 1.9
6	70.3 ± 2.2	64.7 ± 1.4	60.3 ± 3.5	53.2 ± 2.6	64.9 ± 1.4	57.6 ± 2.4	52.2 ± 2.3	48.4 ± 1.3
7	56.3 ± 1.8	53.2 ± 1.5	50.7 ± 0.7	44.8 ± 1.3	57.3 ± 2.2	52.9 ± 2.2	46.4 ± 2.2	39.9 ± 2.6
8	67.9 ± 2.4	62.0 ± 3.0	56.7 ± 2.1	53.1 ± 2.1	64.3 ± 1.9	56.6 ± 2.2	51.8 ± 1.9	45.5 ± 1.7
9	62.5 ± 2.7	57.4 ± 1.6	50.9 ± 1.1	47.6 ± 1.6	78.7 ± 2.1	69.8 ± 1.1	62.0 ± 1.6	55.4 ± 1.4
10	78.2 ± 2.5	67.4 ± 1.1	61.1 ± 2.6	59.9 ± 2.1	59.9 ± 1.1	52.3 ± 3.7	43.7 ± 1.5	36.6 ± 1.5
11	66.9 ± 1.9	60.9 ± 1.2	57.6 ± 2.8	53.1 ± 2.5	67.1 ± 1.2	63.8 ± 2.6	58.8 ± 2.1	54.3 ± 2.2
12	75.4 ± 2.8	70.4 ± 1.4	67.3 ± 2.7	59.6 ± 2.6	52.7 ± 3.1	46.9 ± 1.2	41.4 ± 2.5	38.9 ± 1.8
13	54.7 ± 2.1	51.8 ± 2.4	44.3 ± 2.7	37.8 ± 1.2	50.9 ± 1.1	45.2 ± 0.4	41.6 ± 1.1	34.4 ± 1.6
Vincristine[b]	74.5 ± 2.9	72.6 ± 3.1	70.9 ±2.4	69.8 ± 1.9	74.5 ± 2.9	72.6 ± 3.1	70.9 ±2.4	69.8 ± 1.9

a) See Schme 1 for compounds numbering. b) Standard drug

3.8. Antileishmanial activity

Table 12 describes the antileishmanial activity data of the evaluated compounds using amphotericin B as a standard drug. The data shows that compound 10 caused maximum inhibition activity against *L. tropica* whereas the minimum inhibition is shown by **NaL**. Amphotericin B has shown an effective growth inhibition. It is clearly concluded from the results that organotin(IV) carboxylates show more inhibition of promastigote of *Leishmania tropica* compared to **HL** and **NaL**. The inhibition of promastigote of *Leishmania tropica* activity of the tested compounds may be due the interference with the function of parasite mitochondria [48].

Table 12: Antileishmanial activity data of the synthesized compounds[a]

Comp. No	Dose Conc. (µM)			
	100	**10**	**1**	**0.1**
HL	54.3 ± 1.7	50.2 ± 1.7	44.2 ± 1.9	36.8 ± 2.1
NaL	47.5 ± 1.2	43.8 ± 2.2	40.8 ± 1.4	34.4 ± 2.1
1	71.9 ± 3.2	67.3 ± 2.2	63.2 ± 2.2	57.3 ± 1.4
2	69.6 ± 2.0	65.5 ± 3.3	62.4 ± 1.4	55.8 ± 1.4
3	53.1 ± 2.8	51.6 ± 1.5	46.3 ± 2.1	44.4 ± 1.3
4	59.8 ± 2.7	54.4 ± 2.4	51.3 ± 2.5	44.8 ± 2.1
5	57.2 ± 2.3	52.6 ± 3.1	47.9 ± 1.3	43.2 ± 2.8
6	70.3 ± 3.5	65.6 ± 1.6	62.7 ± 1.6	54.8 ± 1.3
7	77.3 ± 2.1	72.1 ± 2.4	67.9 ± 2.2	61.3 ± 1.5
8	72.7 ± 2.1	64.5 ± 2.5	59.9 ± 3.0	55.3 ± 2.3
9	62.5 ± 2.1	59.8 ± 2.5	55.6 ± 2.1	48.9 ± 1.6
10	78.2 ± 2.2	74.3 ± 3.2	70.7 ± 1.7	62.1 ± 1.6
11	42.1 ± 2.4	37.8 ± 1.1	32.7 ± 1.5	26.7 ± 1.7
12	54.6 ± 3.2	52.1 ± 1.7	50.8 ± 1.4	49.3 ± 1.5

13	63.4 ± 2.2	61.2 ± 2.1	57.4 ± 1.3	50.8 ± 1.4
Amphotericin B[b]	79.8 ± 1.8	76.3 ± 1.4	74.8 ± 2.7	69.9 ± 2.3

a) See Schme 1 for compounds numbering. b) Standard drug

3.9. Antibacterial activity results

Antibacterial activity data against seven pathogenic bacterial strains; *E. coli, S. marcesscens, K. pneumonia, S. epidermidis, S. pyogenes, P. aeruginosa and S. aureus* is given in Table 13. The data shows that only HL and NaL are inactive against the studied bacterial strains while almost all of the complexes possess antibacterial activity. Among the tested complexes only **2**, **6**, **7**, **12** and **13** are active against all the seven bacterial strains. Complexes (**1-13**) are active against *E. coli*, *P. aeruginosa* and *S. aureus* strains. Only complex **1** is inactive against *S. pyogenes* while the remaining **2-13** complexes are active.

Thus the *in vitro* antibacterial study shows that that some of the tested compounds are active against all the bacterial strains so they might be used as potent antibacterial agents after *in vivo* evaluation.

Table 13: Antibacterial activity[a] of the synthesized compounds[b]

Pathogens used→ Comp. No ↓	***E. coli***	***S. marcesscens***	***K. pneumoniae***	***S. epidermidis***	***S. pyogenes***	***P. aeruginosa***	***S. aureus***
	Zone of inhibition in mm (Mean±Standard deviation)						
HL	R	R	R	R	R	R	R
NaL	R	R	R	R	R	R	R
1	7.0±0.0	R	R	R	R	5.0±0.0	5.0±0.0
2	23.0±0.0	15.0±0.0	26.0±0.0	26.0±0.0	20.0±0.0	7.0±0.0	7.0±0.0
3	12.0±0.0	R	R	R	2.0±0.0	12.0±1.7	17.3±0.5
4	20.0±0.0	5.0±0.0	R	20.0±0.0	10.0±0.0	14.6±0.5	20.0±0.0
5	7.0±0.0	R	R	R	19.3±1.1	15.0±0.0	15.0±0.0
6	23.0±0.0	15.0±0.0	25.0±0.0	15.0±0.0	15.0±0.0	15.0±0.0	17.0±3.4
7	17.0±0.0	15.0±0.0	19.0±1.7	8.0±0.0	15.0±0.0	10.0±0.0	10.0±0.0
8	22.0±0.0	R	R	10.0±0.0	7.0±1.0	10.0±0.0	10.0±0.0
9	16.0±0.0	4.0±0.0	-	10.3±0.5	10.0±0.0	9.0±0.0	10.0±0.0
10	9.0±0.0	R	R	R	5.0±0.0	5.0±0.0	5.0±0.0
11	14.0±0.0	R	R	10.0±0.0	7.3±0.5	5.0±0.0	5.6±1.1
12	23.0±0.0	R	14.0±1.7	10.0±0.0	12.0±1.0	17.3±2.5	4.3±1.1
13	23.0±0.0	16.6±2.8	26.0±0.0	26.0±0.0	20.0±0.0	25.0±0.0	26.0±0.0

a) Growth of inhibition were expressed as (0) for no sensitivity, (below 12 mm) for low sensitivity, (12-29 mm) for moderate sensitivity and (30-45 mm) for high sensitivity. **R** indicates (resistant, means have no effect on the test bacterial strain). b) See Schme 1 for compounds numbering.

3.10. Molecular docking results

To assess the interactions of the synthesized compounds with DNA, docking studies were carried out. From the docking study, it was observed that the top ranked conformations of almost all compounds were well interacted with the active residues of the DNA. Among the synthesized compounds, the most active compound is compound **6** on the basis of the docking scores. The docking data explored that the evaluated compounds bind to DNA by intercalation, which is the only interaction mode we obtained by docking. The result of docking of compound **6** with DNA is shown in Fig. 11. It is clear from this figure that the compound **6** showed intercalation with DNA by forming one H bond with chain A, between the oxygen atom of carbonyl group and nitrogen atom of the (G10) guanine whereas carbon of the methoxy moiety of the compound formed H-pi linkage with the guanine (G10) active residue of the DNA. The length of hydrogen bond acceptor formed was found to be 2.37 Å whereas the docking score of the DNA-compound adduct was **-11.7095** (Table 14). Active residue adenine (A17) formed H-donor interaction with the nitrogen atom of the compound while active residue C15 (cytosine) of the DNA made H-pi contact with carbon atom of the methoxy moiety of the inhibitor. Metallo intercalators, transition metal complexes which bind DNA primarily by intercalation, are considered as the most effective class of molecules in these applications [49-51].

Table 14: Docking scores and report of predicted interactions of docked compounds[a] against double stranded DNA

S.No	Interaction details						Docking score
	Ligands	Receptor	Residue	Interaction	Distance	E (kcal/mol)	
HL	C14	O4'	DC 11	H-donor	2.95	-0.9	-9.5593
	O13	N2	DG 16	H-acceptor	2.83	-1.6	
	O20	C5'	DG 12	H-acceptor	3.04	-1.0	
NaL	C 4	O2	DC 15	H-donor	2.87	-0.9	-9.5810
	O23	O4'	DG 10	H-donor	2.45	-3.3	
	O19	C1'	DG 10	H-acceptor	3.26	-0.5	
1	N1	OP1	DC 11	H-donor	2.85	-7.5	-9.4262
	C14	OP1	DC 11	H-donor	3.27	-0.9	
2	O19	C1'	DC 9	H-acceptor	2.87	-0.5	-8.3424
3	O20	C4'	DG10	H-acceptor	3.19	-0.8	-8.5096
4	O13	C5'	DG16	H-acceptor	2.73	-0.9	-8.9695
	O19	C1'	DC15	H-acceptor	3.19	-0.6	
5	C14	OP1	DA 17	H-donor	3.57	-0.5	-8.9332
6	N1	OP1	DA 17	H-donor	2.01	-5.1	-11.7095
	O30	N2'	DG 10	H-acceptor	2.37	-1.3	
	C49	6-ring	DC 15	H-pi	4.74	-0.6	
	C60	5-ring	DG 10	H-pi	4.26	-1.4	
7	C14	OP1	DA 17	H-donor	3.32	-1.5	-8.4210
	6-ring	C5'	DG 12	pi-H	4.29	-0.5	
8	C35	O4'	DA 5	H-donor	3.25	-0.7	-8.2059
	O30	C4'	DA 6	H-acceptor	2.71	-0.9	
9	N1	OP1	DG 10	H-donor	2.89	-3.7	-8.2013
	O13	C5'	DT 19	H-acceptor	2.76	-1.1	
10	C25	O3'	DA 5	H-donor	3.18	-0.8	-9.1031
	N31	OP1	DA 6	H-donor	2.88	-7.9	
	O53	C5'	DG 4	H-acceptor	3.12	-0.7	
11	C43	OP1	DG 4	H-donor	2.82	-1.1	-7.7331
12	C9	O4	DT 20	H-donor	3.49	-0.5	-8.1089
	C41	OP2	DA 17	H-donor	3.58	-0.7	
13	O52	N6	DA 18	H-acceptor	3.02	-3.1	-7.2091

a) See Schme 1 for compounds numbering

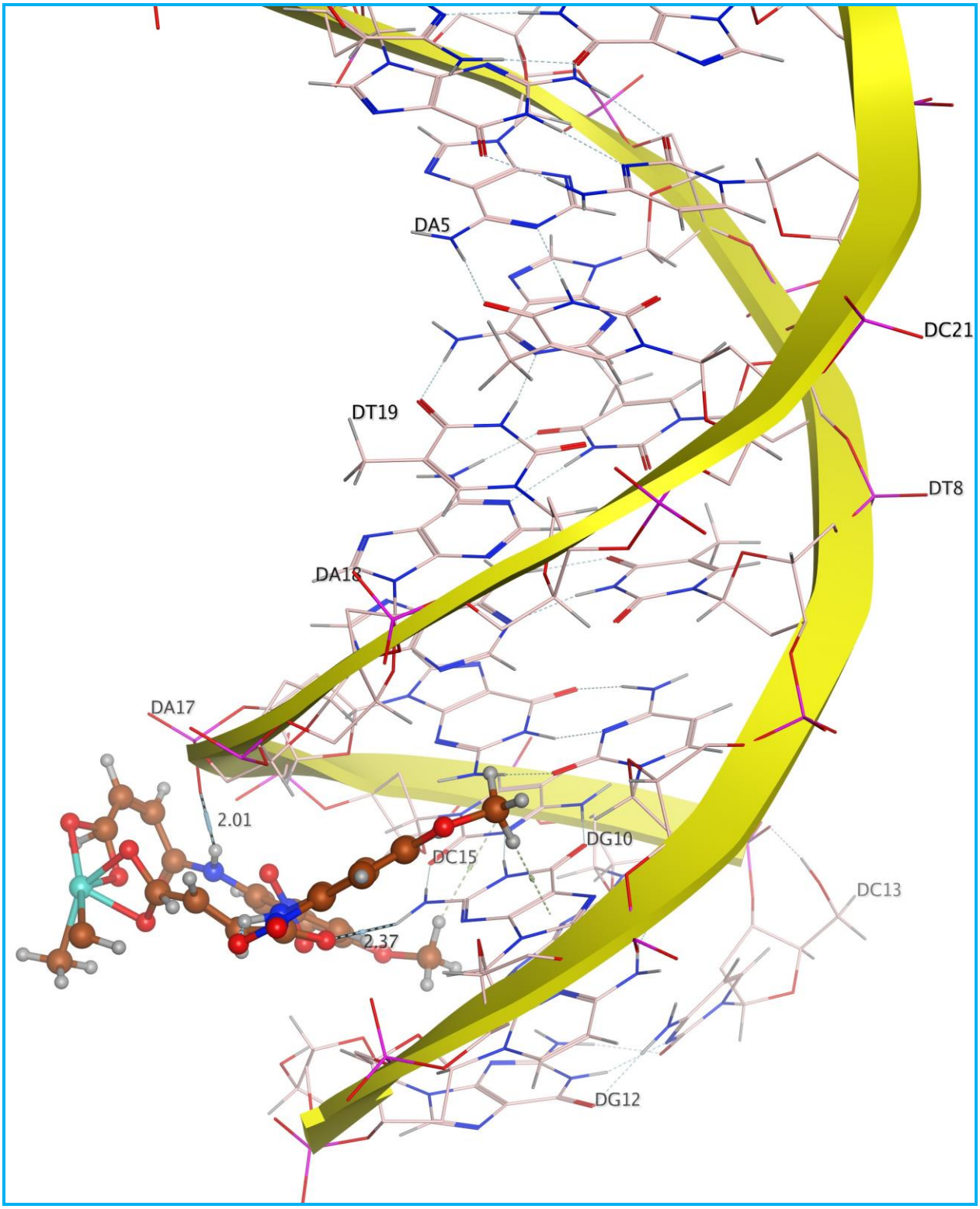

Fig. 11: Molecular docked structure of the compound **6** with DNA.

Conclusions

Thirteen new carboxylate based organotin(IV) complexes were successfully synthesized and characterized by a number of spectroscopic techniques including FT-IR, NMR, XRD and mass spectrometry. The ligand, (*E*)-4-((4-methoxy-2-nitrophenyl)amino)-4-oxobut-2-enoic acid, was prepared in good yield by an economical method in a very short time of just 3-5 minutes in glacial acetic acid. Both solid and solution states chemistry revealed that the (*E*)-4-((4-methoxy-2-nitrophenyl)amino)-4-oxobut-2-enoic acid molecule attaches to the tin atom through oxygen atoms of the COO^- moiety. Multinuclear NMR results propose a penta-coordinated trigonal bipyramidal and hexa-coordinated octahedral geometries for tri- and di-organotin(IV) derivatives, respectively. Results of spectroscopic elucidation were also enhanced by the single crystal XRD data. The results of both the experimentally performed binding study with DNA and theoretically conducted by molecular docking study demonstrate the intercalative mode of interaction of the compounds with DNA. The significant cytotoxicity against the tested cancerous cell lines has explored the anticancer potential of evaluated compounds. Excellent results were obtained in case of antileishmanial activity as activity of some compounds is very close to that of amphotericin B which was used as standard. The antibacterial results of the evaluated compounds suggest them as good antibacterial agents.

Acknowledgment

Grant No. 6796/KPK/NRPU/R&D/HEC/2016 awarded by Higher Education Commission Islamabad Pakistan is highly acknowledged by Muhammad Sirajuddin.

References

[1] N. Naz, M. Sirajuddin, A. Haider, S.M. Abbas, S. Ali, A. Wadood, M. Ghufran, G. Rehman, B. Mirza, Synthesis, characterization, biological screenings and molecular docking study of Organotin (IV) derivatives of 2, 4-dichlorophenoxyacetic acid, Journal of Molecular Structure, 1179 (2019) 662-671.

[2] M. Sirajuddin, M. Tariq, S. Ali, Organotin (IV) carboxylates as an effective catalyst for the conversion of corn oil into biodiesel, Journal of Organometallic Chemistry, 779 (2015) 30-38.

[3] M. Tariq, N. Muhammad, M. Sirajuddin, S. Ali, N.A. Shah, N. Khalid, M.N. Tahir, M.R. Khan, Synthesis, spectroscopic characterization, X-ray structures, biological screenings, DNA

interaction study and catalytic activity of organotin (IV) 3-(4-flourophenyl)-2-methylacrylic acid derivatives, Journal of Organometallic Chemistry, 723 (2013) 79-89.
[4] M. Tariq, S. Ali, N. Muhammad, N.A. Shah, M. Sirajuddin, M.N. Tahir, N. Khalid, M.R. Khan, Biological screening, DNA interaction studies, and catalytic activity of organotin (IV) 2-(4-ethylbenzylidene) butanoic acid derivatives: synthesis, spectroscopic characterization, and X-ray structure, Journal of Coordination Chemistry, 67 (2014) 323-340.
[5] B. Radke, M. Staniszewska, A. Wasik, J. Namieśnik, J. Bolałek, Organotin Compounds in Marine Sediments, Polish Journal of Environmental Studies, 17 (2008).
[6] K. Jamil, R. Wajid, M. Bakhtiar, M. Danish, Biologically active organotin (IV) schiff base complexes, Journal of the Iranian Chemical Society, 7 (2010) 495-499.
[7] R. Yasmeen, M. Adeel, B. Muhammad, F. Rahim, Synthesis Structural Verification and Biological Screening of Some Tin (IV) Dithiocarbamates, Journal of the Chemical Society of Pakistan, 35 (2013) 487-495.
[8] I. Omae, Organotin antifouling paints and their alternatives, Applied organometallic chemistry, 17 (2003) 81-105.
[9] D. Park, J.A. Finlay, R.J. Ward, C.J. Weinman, S. Krishnan, M. Paik, K.E. Sohn, M.E. Callow, J.A. Callow, D.L. Handlin, Antimicrobial behavior of semifluorinated-quaternized triblock copolymers against airborne and marine microorganisms, ACS applied materials & interfaces, 2 (2010) 703-711.
[10] E.R. Tiekink, Tin dithiocarbamates: applications and structures, Applied Organometallic Chemistry, 22 (2008) 533-550.
[11] J. Devi, S. Pachwania, Recent advancements in DNA interaction studies of organotin (IV) complexes, Inorganic Chemistry Communications, (2018).
[12] W. Rehman, R. Yasmeen, F. Rahim, M. Waseem, C.-Y. Guo, Z. Hassan, U. Rashid, K. Ayub, Synthesis biological screening and molecular docking studies of some tin (IV) Schiff base adducts, Journal of Photochemistry and Photobiology B: Biology, 164 (2016) 65-72.
[13] I. Ali, M. Nadeem Lone, Z. A Al-Othman, A. Al-Warthan, M. Marsin Sanagi, Heterocyclic scaffolds: centrality in anticancer drug development, Current drug targets, 16 (2015) 711-734.

[14] M. Iqbal, S. Ali, A. Haider, N. Khalid, Therapeutic properties of organotin complexes with reference to their structural and environmental features, Reviews in Inorganic Chemistry, 37 (2017) 51-70.
[15] P. Zhang, P.J. Sadler, Advances in the design of organometallic anticancer complexes, Journal of Organometallic Chemistry, 839 (2017) 5-14.
[16] I. Ali, M.N. Lone, Z.A. Alothman, A. Alwarthan, Insights into the pharmacology of new heterocycles embedded with oxopyrrolidine rings: DNA binding, molecular docking, and anticancer studies, Journal of molecular liquids, 234 (2017) 391-402.
[17] F. Barbieri, M. Viale, F. Sparatore, G. Schettini, A. Favre, C. Bruzzo, F. Novelli, A. Alama, Antitumor activity of a new orally active organotin compound: a preliminary study in murine tumor models, Anti-cancer drugs, 13 (2002) 599-604.
[18] M. Sirajuddin, S. Ali, A. Badshah, Drug–DNA interactions and their study by UV–Visible, fluorescence spectroscopies and cyclic voltametry, Journal of Photochemistry and Photobiology B: Biology, 124 (2013) 1-19.
[19] W.L. Armarego, Purification of laboratory chemicals, Butterworth-Heinemann, 2017.
[20] K. Sisido, Y. Takeda, Z. Kinugawa, Direct synthesis of organotin compounds. I. Di-and tribenzyltin chlorides, Journal of the American Chemical Society, 83 (1961) 538-541.
[21] M. Sirajuddin, S. Ali, V. McKee, H. Ullah, Synthesis, spectroscopic characterization and in vitro antimicrobial, anticancer and antileishmanial activities as well interaction with Salmon sperm DNA of newly synthesized carboxylic acid derivative, 4-(4-methoxy-2-nitrophenylamino)-4-oxobutanoic acid, Spectrochimica Acta Part A: Molecular and Biomolecular Spectroscopy, 138 (2015) 569-578.
[22] M. Sirajuddin, S. Ali, V. McKee, S. Zaib, J. Iqbal, Organotin (IV) carboxylate derivatives as a new addition to anticancer and antileishmanial agents: design, physicochemical characterization and interaction with Salmon sperm DNA, RSC Advances, 4 (2014) 57505-57521.
[23] S. Murtaza, S. Shamim, N. Kousar, M.N. Tahir, M. Sirajuddin, U.A. Rana, Synthesis, biological investigation, calf thymus DNA binding and docking studies of the sulfonyl hydrazides and their derivatives, Journal of Molecular Structure, 1107 (2016) 99-108.

[24] A. Abbas, S. Murtaza, M.N. Tahir, S. Shamim, M. Sirajuddin, U.A. Rana, K. Naseem, H. Rafique, Synthesis, antioxidant, enzyme inhibition and DNA binding studies of novel N-benzylated derivatives of sulfonamide, Journal of Molecular Structure, 1117 (2016) 269-275.
[25] P. Skehan, R. Storeng, D. Scudiero, A. Monks, J. McMahon, D. Vistica, J.T. Warren, H. Bokesch, S. Kenney, M.R. Boyd, New colorimetric cytotoxicity assay for anticancer-drug screening, JNCI: Journal of the National Cancer Institute, 82 (1990) 1107-1112.
[26] K. Araki-Sasaki, S. Aizawa, M. Hiramoto, M. Nakamura, O. Iwase, K. Nakata, Y. Sasaki, T. Mano, H. Handa, Y. Tano, Substance P-induced cadherin expression and its signal transduction in a cloned human corneal epithelial cell line, Journal of cellular physiology, 182 (2000) 189-195.
[27] S.Z. Imtiaz Khan, Aliya Ibrar, Nasim Hasan Rama, Jim Simpson, Jamshed Iqbal, Synthesis, crystal structure and biological evaluation of some novel 1, 2, 4-triazolo [3, 4-b]-1, 3, 4-thiadiazoles and 1, 2, 4-triazolo [3, 4-b]-1, 3, 4-thiadiazines, European journal of medicinal chemistry 78 (2014) 167-177.
[28] M.I. Choudhary, W.J. Thomsen, Bioassay techniques for drug development, CRC Press, 2003.
[29] K.A. Hammer, C. Carson, T. Riley, Antimicrobial activity of essential oils and other plant extracts, Journal of applied microbiology, 86 (1999) 985-990.
[30] C.C.G. Inc., Molecular operating environment (MOE), in, Chemical Computing Group Inc 1010 Sherbooke St. West, Suite# 910, Montreal, QC, Canada, H3A 2R7, 2016.
[31] D. Kovala-Demertzi, V.N. Dokorou, J.P. Jasinski, A. Opolski, J. Wiecek, M. Zervou, M.A. Demertzis, Organotin flufenamates: synthesis, characterization and antiproliferative activity of organotin flufenamates, Journal of organometallic chemistry, 690 (2005) 1800-1806.
[32] M. Nara, H. Torii, M. Tasumi, Correlation between the vibrational frequencies of the carboxylate group and the types of its coordination to a metal ion: an ab initio molecular orbital study, The Journal of Physical Chemistry, 100 (1996) 19812-19817.
[33] V. Zeleňák, Z. Vargová, K. Györyová, Correlation of infrared spectra of zinc (II) carboxylates with their structures, Spectrochimica Acta Part A: Molecular and Biomolecular Spectroscopy, 66 (2007) 262-272.

[34] M. Tariq, M. Sirajuddin, S. Ali, N. Khalid, N. Shah, Biological evaluations and spectroscopic characterizations of 3-(4-ethoxyphenyl)-2-methylacrylate based organotin (IV) carboxylates derivatives, Russian Journal of General Chemistry, 87 (2017) 2690-2698.
[35] T.P. Lockhart, W.F. Manders, E.M. Holt, Solution and solid-state molecular structures of Me2Sn (OAc) 2 and its hydrolyzate,([Me2Sn (OAc)] 2O) 2, by solution and solid-state carbon-13 NMR. X-ray diffraction study of the hydrolyzate, Journal of the American Chemical Society, 108 (1986) 6611-6616.
[36] A. Munir, M. Sirajuddin, M. Zubair, A. Haider, S. Tirmizi, S. Ali, H. Khan, K. Ullah, I. Aziz, Synthesis, spectroscopic characterization, and biological screening of levofloxacin based organotin (IV) derivatives, Russian Journal of General Chemistry, 87 (2017) 2380-2390.
[37] Y. Farina, A. Graisa, E. Yousif, Synthesis, Structure and Biological Activity of Some Diorganotin (IV) with Benzamidomethionine, Modern Applied Science, 3 (2009) 215.
[38] T.P. Lockhart, W.F. Manders, Structure determination by NMR spectroscopy. Dependence of| 2J (119Sn, 1H)| on the Me-Sn-Me angle in methyltin (IV) compounds, Inorganic Chemistry, 25 (1986) 892-895.
[39] W.F. Howard Jr, R.W. Crecely, W.H. Nelson, Octahedral dialkyltin complexes: a multinuclear NMR spectral solution structural study, Inorganic Chemistry, 24 (1985) 2204-2208.
[40] J.J. Burke, P.C. Lauterbur, Sn1 Nuclear Magnetic Resonance Spectra1, Journal of the American Chemical Society, 83 (1961) 326-331.
[41] V. Torocheshnikov, A. Tupčiauskas, Y.A. Ustynyuk, A 119Sn NMR study of tin derivatives of cyclopentadiene, Journal of Organometallic Chemistry, 81 (1974) 351-356.
[42] F.-f. Yan, Q. Zhu, Q.-L. Li, R.-F. Zhang, C.-L. Ma, Triorganotin coordination polymers based on three dicarboxylate ligands containing flexible SS bonds: synthesis, structures and in vitro anti-tumor activity, Journal of Organometallic Chemistry, 880 (2019) 156-162.
[43] F. Shaheen, M. Sirajuddin, S. Ali, P.J. Dyson, A. Haider, M.N. Tahir, K. Shahid, Synthesis, structural elucidation and biological activities of organotin (IV) derivatives of 4-(2-thienyl) butyric acid, Journal of the Iranian Chemical Society, 14 (2017) 387-394.
[44] M. Sirajuddin, S. Ali, V. McKee, M. Sohail, H. Pasha, Potentially bioactive organotin (IV) compounds: synthesis, characterization, in vitro bioactivities and interaction with SS-DNA, European journal of medicinal chemistry, 84 (2014) 343-363.

[45] E.C. Long, J.K. Barton, On demonstrating DNA intercalation, Accounts of Chemical Research, 23 (1990) 271-273.
[46] H.A. Benesi, J. Hildebrand, A spectrophotometric investigation of the interaction of iodine with aromatic hydrocarbons, Journal of the American Chemical Society, 71 (1949) 2703-2707.
[47] N. Ahmad, D.K. Feyes, R. Agarwal, H. Mukhtar, A.-L. Nieminen, Green tea constituent epigallocatechin-3-gallate and induction of apoptosis and cell cycle arrest in human carcinoma cells, Journal of the National Cancer Institute, 89 (1997) 1881-1886.
[48] S. Shahzadi, S. Ali, K. Shahid, M. Yousaf, S.K. Sharma, K. Qanungo, Interaction of Di-and Triorganotin (IV) Compounds with Carboxylate Ligand: Synthesis, Spectral Characterization, Semi-Empirical Study and In Vitro Antimicrobial Activities, Journal of the Chinese Chemical Society, 57 (2010) 659-670.
[49] J.K. Barton, E.D. Olmon, P.A. Sontz, Metal complexes for DNA-mediated charge transport, Coordination chemistry reviews, 255 (2011) 619-634.
[50] T. Biver, F. Secco, M. Venturini, Mechanistic aspects of the interaction of intercalating metal complexes with nucleic acids, Coordination Chemistry Reviews, 252 (2008) 1163-1177.
[51] H.-K. Liu, P.J. Sadler, Metal complexes as DNA intercalators, Accounts of Chemical Research, 44 (2011) 349-359.

Highlights

- Synthesis of novel organotin(IV) carboxylates
- Spectroscopic characterizations and Structural elucidation
- Interaction with SS-DNA *via* intercalative mode of interaction
- *In vitro* antibacterial, anticancer and antileishmanial activity
- Molecular docking